

(2*S*,3*S*)-3-Amino-4-(3,3-difluoropyrrolidin-1-yl)-*N,N*-dimethyl-4-oxo-2-(4-[1,2,4]triazolo[1,5-*a*]pyridin-6-ylphenyl)butanamide: A Selective α -Amino Amide Dipeptidyl Peptidase IV Inhibitor for the Treatment of Type 2 Diabetes

Scott D. Edmondson,^{†,*} Anthony Mastracchio,[†] Robert J. Mathvink,[†] Jiafang He,[†] Bart Harper,[†] You-Jung Park,[†] Maria Beconi,^{||,#} Jerry Di Salvo,[†] George J. Eiermann,[‡] Huaibing He,[†] Barbara Leiting,[§] Joseph F. Leone,[†] Dorothy A. Levorse,[†] Kathryn Lyons,[†] Reshma A. Patel,[§] Sangita B. Patel,[†] Aleksandr Petrov,[‡] Giovanna Scapin,[†] Jackie Shang,^{||} Ranabir Sinha Roy,[§] Aaron Smith,[†] Joseph K. Wu,[§] Shiyao Xu,^{||} Bing Zhu,^{||} Nancy A. Thornberry,[§] and Ann E. Weber[†]

Merck Research Laboratories, Merck & Co., Inc., Rahway, New Jersey 07065

Received January 6, 2006

A series of β -substituted biarylphenylalanine amides were synthesized and evaluated as inhibitors of dipeptidyl peptidase IV (DPP-4) for the treatment of type 2 diabetes. Optimization of the metabolic profile of early analogues led to the discovery of (2*S*,3*S*)-3-amino-4-(3,3-difluoropyrrolidin-1-yl)-*N,N*-dimethyl-4-oxo-2-(4-[1,2,4]triazolo[1,5-*a*]pyridin-6-ylphenyl)butanamide (**6**), a potent, orally active DPP-4 inhibitor (IC₅₀ = 6.3 nM) with excellent selectivity, oral bioavailability in preclinical species, and in vivo efficacy in animal models. Compound **6** was selected for further characterization as a potential new treatment for type 2 diabetes.

Introduction

Inhibition of dipeptidyl peptidase IV (DPP-4)^a has recently emerged as a promising new approach for the treatment of type 2 diabetes mellitus.¹ DPP-4 is the enzyme responsible for inactivation of the incretin hormones glucagon-like peptide 1 (GLP-1) and glucose-dependent insulinotropic polypeptide (GIP). These two hormones are secreted in response to nutrient ingestion, and each enhances the glucose-dependent secretion of insulin. Additionally, GLP-1 has been shown in mammals to stimulate insulin biosynthesis, inhibit glucagon secretion, slow gastric emptying, reduce appetite, and stimulate β -cell neogenesis and differentiation.^{1,2}

Due to rapid processing of GLP-1 and GIP by DPP-4, the half-lives of the active peptides in blood are extremely short. Inhibition of DPP-4 in humans has been shown to increase circulating GLP-1 and GIP levels which lead to decreased blood glucose levels, hemoglobin A_{1c} levels, and glucagon levels.^{2,3c,5c} DPP-4 inhibitors offer a number of potential advantages over existing diabetes therapies including a lowered risk of hypoglycemia, a lowered risk of weight gain, and the potential for the regeneration and differentiation of pancreatic β -cells. Conse-

quently, potent small molecule DPP-4 inhibitors such as vildagliptin (NVP-LAF237, **1**),³ saxagliptin (BMS-477118, **2**),⁴ and sitagliptin (MK-0431, **3**)⁵ (Chart 1) have advanced into late stage human clinical trials.

DPP-4 is a serine protease which cleaves a dipeptide from the N-terminus of GLP-1[7–36] to give an inactive GLP-1[9–36] peptide. Since DPP-4 preferentially cleaves substrates with proline at the P-1 position, it is not surprising that a common structural motif among many DPP-4 inhibitors is a pyrrolidine-bearing electrophile at the P-1 site linked to an α -amino acid at the P-2 site.^{1c} Some of these electrophiles are irreversible inhibitors (phosphonates) while others are reversible (nitriles, boronic acids) inhibitors.^{1c} A potential liability of the reversible inhibitors is poor chemical stability due to the propensity of the free amine group to cyclize with the electrophile thus forming a six-membered ring. Cyanopyrrolidines such as **1** and **2** are representative of this potent class of DPP-4 inhibitors, and each of these compounds has been optimized with respect to chemical stability and potency.^{3,4} An alternative option to access potent and stable DPP-4 inhibitors would be to optimize for increased potency at the P-2 substituent of α -amino acid derivatives lacking an electrophile.⁶

Previous reports from these laboratories describe a series of β -substituted phenylalanine derivatives which lack an electrophile attached to the pyrrolidine ring.⁷ Optimization of the β -substituent of the phenylalanine led to β -dimethylamide **4**, an intrinsically potent DPP-4 inhibitor (IC₅₀ = 12 nM) with a high serum potency shift (32-fold) due to high plasma protein binding.^{7b} Replacement of the 4-fluorophenyl group in the homophenylalanine series with polar heterocycles such as a methylpyridone (**5**) resulted a reduced serum shift and a good pharmacokinetic profile in rats, dogs, and monkeys.⁸ Unfortunately, the methylpyridone moiety is metabolically labile, forming the free pyridone ring upon metabolism. Since this metabolite is also a potent DPP-4 inhibitor and active at various ion channels, further development of **5** was abandoned.

Herein, we describe a series of fused heterocyclic bioisosteres to the methylpyridone moiety that solve the liabilities associated with **5**. Further improvement of the metabolic profile of the (S)-3-fluoropyrrolidine moiety ultimately led to the discovery

* To whom correspondence should be addressed. Scott D. Edmondson, Merck Research Laboratories, Mail Code RY123-234 P.O. Box 2000 Rahway, NJ 07065-0900. Tel: (732) 594-0287. Fax: (732) 594-5350. E-mail: scott_edmondson@merck.com.

[†] Department of Medicinal Chemistry.

[§] Department of Metabolic Disorders.

^{||} Department of Drug Metabolism.

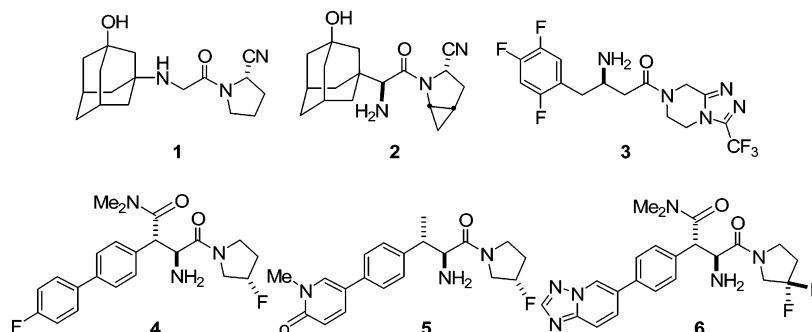
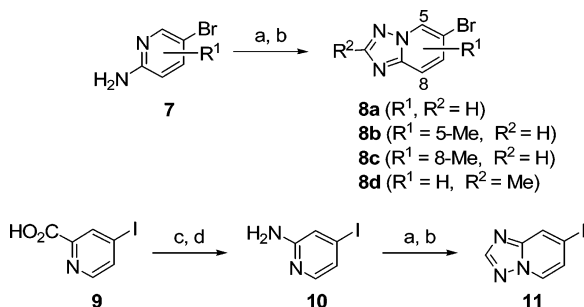
[‡] Department of Pharmacology.

[†] Department of Immunology and Rheumatology.

[#] Current address: GlaxoSmithKline, RI-CEDD, 709 Swedeland Rd., King of Prussia, PA 19406.

^a Nonstandard abbreviations: DPP-4 = dipeptidyl peptidase 4, GLP-1 = glucagon-like peptide 1, GIP = glucose-dependent insulinotropic polypeptide, CBS reagent = 2-methyl-CBS-oxazaborolidine, DPP8 = dipeptidyl peptidase 8, DPP9 = dipeptidyl peptidase 9, FAP = seprase or fibroblast activation protein, QPP = quiescent cell proline dipeptidase, DPP-II = dipeptidyl peptidase II, APP = amino peptidase P, F = oral bioavailability, val-pyr = valine pyrrolidide, SAR = structure–activity relationships, MRT = mean residence time, hERG = human ether-a-go-go which is a human cardiac potassium ion channel, OGTT = oral glucose tolerance test, PD = pharmacodynamic, AMC = aminomethylcoumarin, DIO = diet-induced obese, AUC = area under the curve, and Cl_p = clearance.

Chart 1

Scheme 1^a

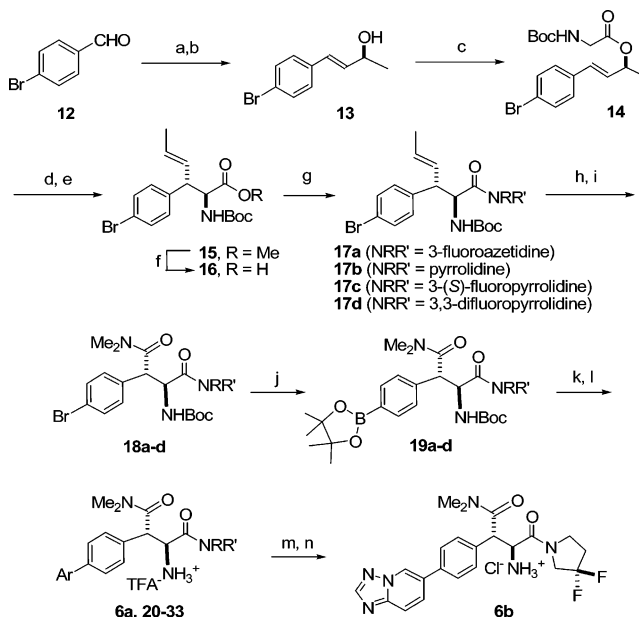
^a Reagents: (a) $\text{Me}_2\text{NCR}^2(\text{OMe})_2$, DMF, 130 °C, 12 h; (b) $\text{H}_2\text{NOSO}_3\text{H}$, MeOH, pyr, 0 °C to room temperature; (c) *t*-BuOH, toluene, Et_3N , DPPA, rt to 100 °C, 4 h; (d) TFA/DCM (1:2), 0 °C to room temperature.

of (2*S*,3*S*)-3-amino-4-(3,3-difluoropyrrolidin-1-yl)-*N,N*-dimethyl-4-oxo-2-(4-[1,2,4]triazolo[1,5-*a*]pyridin-6-ylphenyl)butanamide (**6**), a potent, selective, and orally active DPP-4 inhibitor with an excellent pharmacokinetic profile in four species. This compound was selected for extensive in vivo evaluation for the treatment of type 2 diabetes.

Chemistry

Heterocyclic intermediates **8a–d** and **11** were synthesized following the routes illustrated in Scheme 1. 2-Amino-5-bromopyridines (**7**) were heated with dimethylacetamide dimethylacetal or dimethylpropionamide dimethylacetal in DMF, followed by treatment with hydroxylamine-*O*-sulfonic acid to afford the substituted 6-bromo[1,2,4]triazolo[1,5-*a*]pyridines **8a–d**.⁹ A similar procedure was performed on 2-amino-4-iodopyridine (**10**) to afford triazaole **11**. Aminopyridine **10** was generated via a Curtius rearrangement of acid **9** based on a literature reported sequence.¹⁰

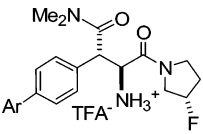
Inhibitors were synthesized using a variation of a route previously described by these laboratories (Scheme 2).^{7b} Horner–Emmons reaction of 4-bromobenzaldehyde (**12**) with diethyl (2-oxopropyl)phosphonate afforded the corresponding trans enone in excellent yield (81%). A chiral reduction of the enone with (*R*)-2-methyl-CBS-oxazaborolidine (*R*-CBS reagent) was next employed to afford the *S*-styrenol **13** in excellent yield (90%) and enantioselectivity (96% ee).¹¹ The assignment of an *S* absolute configuration to alcohol **13** was initially supported by CBS reagent precedent^{11a} and later confirmed by X-ray crystallographic analysis of analogue **23** (vide infra) which was derived from **13**. Enantiomeric excess could be enhanced to >98% ee by recrystallization from cyclohexane. Next, the alcohol was condensed with Boc-glycine under standard conditions to afford ester **14**. Exposure of **14** to Kazmaier's enolate-Claisen rearrangement conditions¹² followed by esterification of the resulting acid with trimethylsilyldiazomethane then afforded *N*-Boc amino ester **15** in excellent yield and stereo-

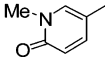
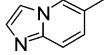
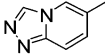
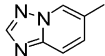
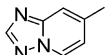
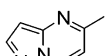
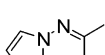
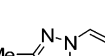

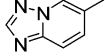
Scheme 2^a

^a Reagents: (a) $(\text{EtO})_2\text{POCH}_2\text{COCH}_3$, DBU, THF; (b) *R*-CBS, catecholborane, toluene, –78 °C to –30 °C; (c) EDC, HOBt, Boc-Gly, DIEA, DCM; (d) LHMDS, ZnCl_2 , THF, –78 °C; (e) TMSCHN_2 , Et_2O , MeOH; (f) 1 N LiOH, THF, MeOH; (g) EDC, $\text{RR}'\text{NH}$, HOBt, DIEA, DCM; (h) KMnO_4 , NaIO₄, K_2CO_3 , *t*-BuOH, H_2O ; (i) EDC, HOBt, Me_2NH , DIEA, DCM; (j) bis(pinacolato)diboron, DMSO, KOAc, $\text{Pd}(\text{dppf})_2\text{Cl}_2$, 80 °C, 4 h; (k) ArX , toluene, EtOH, 2 N aqueous Na_2CO_3 , $\text{Pd}(\text{dppf})_2\text{Cl}_2$, 90 °C, 12 h; (l) TFA, DCM; (m) Na_2CO_3 , H_2O ; (n) HCl, DCM, rt.

selectivity. Esterification to form **15** was performed in order to facilitate purification, and this ester was subsequently saponified to give acid **16** which was used without purification. This combination of a chiral CBS reduction with an enolate Claisen rearrangement is an especially effective method of synthesizing orthogonally functionalized, β -substituted phenylalanine derivatives in high enantiomeric excess.

Next, acid **16** was coupled with 3-fluoroazetidine,¹³ pyrrolidine, (*S*)-3-fluoropyrrolidine,¹⁴ or 3,3-difluoropyrrolidine¹⁴ using standard coupling conditions to give amides **17a–d** in yields of 60–95%. Oxidative cleavage of the olefin to the corresponding acids followed by standard EDC coupling of these acids with dimethylamine then afforded dimethylamides **18a–d** in 50–90% overall yields. Treatment of bromides **18a–d** with bis(pinacolato)diboron under palladium catalysis provided boronates **19a–d** in excellent yields (>80%). Suzuki couplings of boronates **19a–d** with a series of heterocyclic halides afforded the desired coupled products, which were then deprotected under standard conditions to give inhibitors **6** and **20–33** in Tables 1–3 as the trifluoroacetic acid (TFA) salts. The TFA salt **6a** was converted to a hydrochloric acid salt **6b** for in vivo evaluation.

Table 1. Inhibitory Properties (IC₅₀s) of Selected Biarylphenylalanine (*S*)-Fluoropyrrolidide Amides


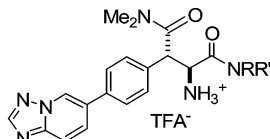
Compd	Ar	DPP-4 ^a (nM)	+50% HS ^b (nM)	QPP (nM)	DPP8 (nM)	DPP9 (nM)
4 ^c	4-FPh	12	387	45,000	>100,000	>100,000
20		8.0	79	>100,000	>100,000	>100,000
21		13	133 ^d	>100,000	>100,000	>100,000
22		4.1 ^e	16	>100,000	>100,000	>100,000
23		4.3	44	>100,000	>100,000	>100,000
24		5.3	35	14,000	>100,000	>100,000
25		8.0	53	63,000	>100,000	>100,000
26		13	177	>100,000	>100,000	>100,000
27		22	223	>100,000	>100,000	>100,000
28		8.6	61	>100,000	>100,000	>100,000
29		150	640 ^d	>100,000	>100,000	>100,000

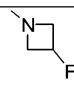
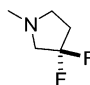
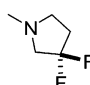
^a Unless otherwise noted, values reported are the mean of a minimum of two experiments with a standard deviation <25% of the mean. ^b Assay done in the presence of 50% human serum. Unless otherwise noted, values reported are the mean of a minimum of two experiments with a standard deviation <40% of the mean. ^c Values reported for compound **4** are taken from ref 7b. ^d Values reported are the results of a single experiment. ^e Value is 4.1 ± 3.6 nM.

Results and Discussion

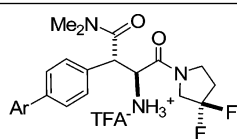
Compounds **6a** and **20–33** were evaluated for in vitro inhibition of DPP-4.¹⁵ As a surrogate measure of plasma protein binding, each inhibitor was also measured for DPP-4 inhibition in the presence of 50% human serum.^{7b} Each inhibitor was also tested against DPP8,¹⁶ DPP9,¹⁷ FAP (seprase),¹⁸ and other proline specific enzymes with DPP-4 like activity,¹⁹ including QPP (DPP-II),^{15,20} amino peptidase P (APP), and prolidase. Selectivity over DPP8 and DPP9 was considered particularly important because inhibition of these enzymes has been associated with toxicity in preclinical species and their relevance to humans is not yet known.²¹ Consequently, inhibition data for each compound against DPP8 and DPP9 is presented in Table 1. With the exception of QPP (data also presented), inhibition of the other enzymes was weak (IC₅₀s > 40,000 nM).

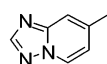
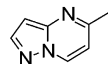
DPP-4 inhibitory activities for selected (*S*)-3-fluoropyrrolidide-derived analogues are listed in Table 1. For comparison, fluorophenyl derivative **4** is also included in the table. Although methylpyridone **20** is similar to **4** in terms of intrinsic DPP-4 potency, **20** exhibited only a 10-fold serum potency shift compared to a 32-fold shift observed with **4**. To address the possibility of metabolic demethylation of the *N*-methylpyridone ring, a series of fused heterocycles (i.e. **21–26**) was generated which was expected to mimic the stereoelectronic effect of the methylpyridone moiety. Heterocycles **21–26** were all comparable to **20** in terms of intrinsic potency, but **21** and **26** suffer from large serum potency shifts. Pharmacokinetic evaluation of **20** and **22–25** (IC₅₀s < 10 nM) in the rat revealed that **20** and **22** suffered from low oral bioavailabilities ($F_{\text{rat}} < 3\%$, Table 4) while **24** displayed a moderate oral bioavailability ($F_{\text{rat}} = 21\%$).

Table 2. Inhibitory Properties (IC_{50} s) of Selected Biarylphenylalanine Amides


Compd	-NRR'	DPP-4 ^a (nM)	+50% HS ^b (nM)	QPP (nM)	DPP8 (nM)	DPP9 (nM)
30		2.7	41 ^c	>100,000	>100,000	>100,000
31	-N(CH ₂) ₄	5.2	63	>100,000	>100,000	14,000
6a		6.3	71	61,000	>100,000	>100,000
6b		8.8	55	>100,000	>100,000	>100,000

^a Unless otherwise noted, values reported are the mean of a minimum of two experiments with a standard deviation <25% of the mean. ^b Assay done in the presence of 50% human serum. Unless otherwise noted, values reported are the mean of a minimum of two experiments with a standard deviation <40% of the mean. ^c Values reported are the results of a single experiment.

Table 3. Inhibitory Properties (IC_{50} s) of Selected Biarylphenylalanine Difluoropyrrolidides


Compd	Ar	DPP-4 ^a (nM)	+50% HS ^b (nM)	QPP (nM)	DPP8 (nM)	DPP9 (nM)
32		6.2	34	26,000	>100,000	>100,000
33		7.5	57	18,000	>100,000	>100,000

^a Unless otherwise noted, values reported are the mean of a minimum of two experiments with a standard deviation <25% of the mean. ^b Assay done in the presence of 50% human serum. Unless otherwise noted, values reported are the mean of a minimum of two experiments with a standard deviation <40% of the mean.

Heterocycles **23** and **25**, however, afforded the highest oral bioavailabilities and longest half-lives in the series ($F_{rat} = 43\%$ and 46% ; $t_{1/2} = 2.0$ and 4.3 h respectively).

The X-ray crystal structure determination of triazole **23** ($IC_{50} = 4.3$ nM) bound to the active site of DPP-4 is shown in Figure 1. Compound **23** (yellow) shows significant overlap with a previously reported α -amino acid-derived DPP-4 inhibitor, valine pyrrolidide²² (val-pyr green in Figure 1, DPP-4 $IC_{50} = 1580$ nM). The pyrrolidines of both inhibitors occupy the S1 hydrophobic pocket, and the carbonyls linked to the pyrrolidines are within hydrogen bonding distance from the side chain of Asn710. Furthermore, the amino group of both inhibitors hydrogen bond to the side chains of Tyr662, Glu205, and Glu206. In contrast to val-pyr, the larger compound **23** extends into the S2 pocket, where the dimethyl amide carbonyl forms a hydrogen bond with the side chain of Tyr547. A comparison of the intrinsic potency of β -methylphenylalanine derivative **5**

($IC_{50} = 34$ nM)⁸ with compound **20** ($IC_{50} = 8.0$ nM) is illustrative of the potency enhancement afforded by the dimethyl amide moiety. The central phenyl group appears to provide a sufficient tether length to position the triazolopyridine heterocycle proximal to Arg358. The fused triazole ring stacks against the side chain of Phe357 and hydrogen bonds with the side chain of Arg358. Moreover, SAR trends of analogous phenylalanine-derived DPP-4 inhibitors illustrate the potency enhancing effect of aromatic functionality positioned to interact with Arg358 and Tyr547.⁶⁻⁸ The presence of these additional interactions with the enzyme affords **23** a greater than 350-fold improvement in potency compared to val-pyr.

Due to the excellent DPP-4 potency and rat pharmacokinetic profile of **23**, additional SAR surrounding this compound was explored. Consistent with the X-ray crystal structure, the introduction of methyl substituents on the fused triazole ring system afforded compounds with reduced intrinsic potency (e.g.

Table 4. Pharmacokinetic Profiles of Selected DPP-4 Inhibitors^a

compd	species	Cl _p (mL/min/kg)	t _{1/2} (h)	PO AUC _{norm} (μM·h/mpk)	PO C _{max} (μM)	F (%)
20	rat	15	1.2	0.048	0.021	2
22	rat	34	1.1	0.009	0.008	0.76
23	rat	7.0	2.0	2.4	2.3	43
	dog	3.1	2.4	12	6.6	94
24	rat	10.0	1.7	0.83	0.60	21
25	rat	3.3	4.3	5.6	3.9	46
30	rat	7.3	2.1	2.2	2.4	37
	dog	6.1	2.0	6.9	4.0	100
31	rat	7.7	1.6	2.9	2.1	46
	dog	5.9	1.1	6.8	5.9	98
6a	rat	2.8	1.6	15	6.9	100
	dog	1.8	4.8	16	6.3	73
	monkey	5.3	6.3	4.0	2.8	56
	mouse	1.2	6.7	23	11	68
32	rat	1.8	1.1	15	7.8	69
	dog	1.5	3.4 ^b	20	9.5	81
33	rat	1.4	2.7	24	8.9	79
	dog	1.0	3.1 ^b	38	22	100

^aDose: iv: 1 mpk, po: 2 mpk. ^bValues are for mean residence time (MRT) since t_{1/2} could not be calculated due to secondary peaks in the plasma concentration time profile.

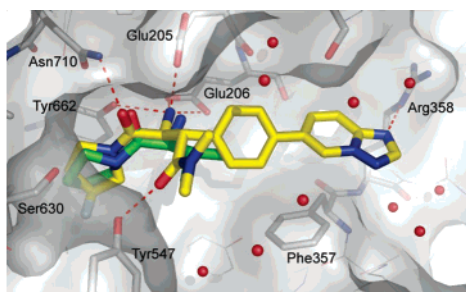


Figure 1. Compound **23** bound to DPP-4. The overlay of compound **23** (yellow) and the substrate analogue valine-pyrrolidine (green, 1N1M.pdb) shows the similar orientation between the two compounds. Interactions of compound **23** with DPP-4 are shown as red dotted lines. The extensive hydrogen bond network present between the ordered water molecules, compound **23**, and protein atoms has been omitted for clarity.

27 and **29**) and increased serum shifts relative to the parent compound **23**.

Potential substitutes for the (*S*)-3-fluoropyrrolidine ring of **23** were next evaluated (Table 2). Fluoroazetidine **30** afforded the best intrinsic potency (DPP-4 IC₅₀ = 2.7 nM) in this series with a 15-fold serum shift. Pyrrolidide **31** (IC₅₀ = 5.2 nM) and difluoropyrrolidide **6a** (IC₅₀ = 6.3 nM) also maintained excellent DPP-4 potency, with serum shifts of 12-fold and 11-fold, respectively. Rat pharmacokinetic evaluation of these three compounds revealed that **30** and **31** each presented a profile similar to that of **23** while incorporation of the difluoropyrrolidine group (**6a**) increased the oral bioavailability substantially (*F*_{rat} = 100%). Further pharmacokinetic evaluation of **23**, **30**, **31**, and **6a** in the dog revealed another potential advantage of the difluoropyrrolidine. While the half-lives of **23**, **30**, and **31** were all less than 2.5 h, the half-life of **6a** was 4.8 h.

Since the (*S*)-3-fluoropyrrolidine moiety in previously reported DPP-4 inhibitors has been demonstrated to be a labile site for metabolic activation, **23** was evaluated for the formation of reactive metabolites in the presence of rat and human liver microsomes.^{23,24} Compound **23** displayed a moderate potential for metabolic activation in both species, with levels of covalent binding due to reactive metabolites measuring 142 pmol/mg protein and 116 pmol/mg of protein in rat and human liver microsomes, respectively. In comparison, compound **6a** showed relatively low levels of covalent binding (less than 50 pmol/

Table 5. Ion Channel Activities (IC₅₀s) of Analogues **6a**, **32**, and **33**

compd	Ca (μM)	hERG (μM)	Na (μM)
6a	>100	>100	>100
32	54	16	>100
33	15	>100	60

mg of protein) in both rat and human liver microsomes, revealing a lower propensity to form reactive metabolites.

The superior metabolic profile and rat oral bioavailability of **6a** relative to **23** suggested that incorporation of the difluoropyrrolidine ring into analogues **24** and **25** might improve their rat oral bioavailabilities. Compounds **32** and **33** (Table 3) each exhibit excellent intrinsic inhibition of DPP-4 (IC₅₀s = 6.2 nM and 7.5 nM, respectively) with a reduced serum shift (5-fold and 8-fold, respectively) relative to **6a** (11-fold). As expected, each these analogues also possess improved oral bioavailabilities (*F*_{rat} = 69% for **32** and 79% for **33**) in the rat relative to their (*S*)-3-fluoropyrrolidine-derived counterparts. The dog pharmacokinetic profiles of **32** and **33** revealed excellent oral bioavailabilities (*F*_{dog} = 81% and 100% respectively) but mean residence times (MRT)²⁵ for **32** (3.4 h) and **33** (3.1 h) shorter than the half-life and MRT for **6a** (t_{1/2} = 4.8 h, MRT = 5.6 h).

Next, binding at hERG,²⁶ human cardiac sodium channel,²⁷ and rabbit calcium channel²⁸ was measured as a general indicator of ion channel activities (Table 5). Although compound **6a** was inactive at each of these ion channels (IC₅₀s > 100 μM), compound **32** showed activity at the potassium channel (hERG IC₅₀ = 16 μM) and **33** exhibited activity at the calcium channel (Ca²⁺ IC₅₀ = 15 μM). Additional in vitro profiling of **6a** in an extensive panel of receptor and ion channel binding and enzyme inhibition assays showed no significant activity at 10 μM (data not shown). Moreover, **6a** also displays excellent pharmacokinetic profiles in the mouse (*F* = 68%, t_{1/2} = 6.7 h) and rhesus monkey (*F* = 56%, t_{1/2} = 6.3 h).

On the basis of an excellent off-target selectivity profile and pharmacokinetic profile in four species, compound **6** was chosen for further in vivo evaluation. The hydrochloride salt **6b** was assessed for its ability to improve glucose tolerance in lean mice. Administration of single oral doses reduced the blood glucose excursion in an oral glucose tolerance test (OGTT) in a dose-dependent manner from 0.1 mg/kg (43% reduction) to 3.0 mg/kg (56% reduction) when administered 60 min before an oral dextrose challenge (5 g/kg, Figure 2). In a separate OGTT experiment, the pharmacodynamic profile of compound **6b** was assessed. Plasma DPP-4 inhibition, compound concentration, and active GLP-1 levels were measured 10 min after dextrose challenge (Figure 3). At the 0.1 mg/kg dose, the plasma concentration of **6** was 269 nM and the reduction of blood glucose excursion corresponded to a 56% inhibition of plasma DPP-4 activity.²⁹ A dosage of 0.3 mg/kg corresponded to a plasma concentration of 1390 nM and provided 83% inhibition of DPP-4. Maximal efficacy resulted in a 2 to 3-fold increase in active GLP-1, analogous to GLP-1 levels observed upon glucose challenge in DPP-4 deficient mice.³⁰ The observed levels of DPP-4 inhibition in the PD assay do not, however, correspond to the expected efficacy of **6b** in light of the intrinsic murine potency (mouse IC₅₀ = 6.0 nM). To resolve this disconnect between in vitro potency and in vivo efficacy, noncovalent plasma protein binding of **6** was measured (Table 6). Since compound **6** is 96% protein bound in the mouse, a free fraction of only 4% is available in the plasma for DPP-4 inhibition. At the 0.1 mg/kg dose in the mouse, 4% of the total plasma concentration of **6** (269 nM) corresponds to a free fraction concentration of only 11 nM. Since the 0.1 mg/kg dose

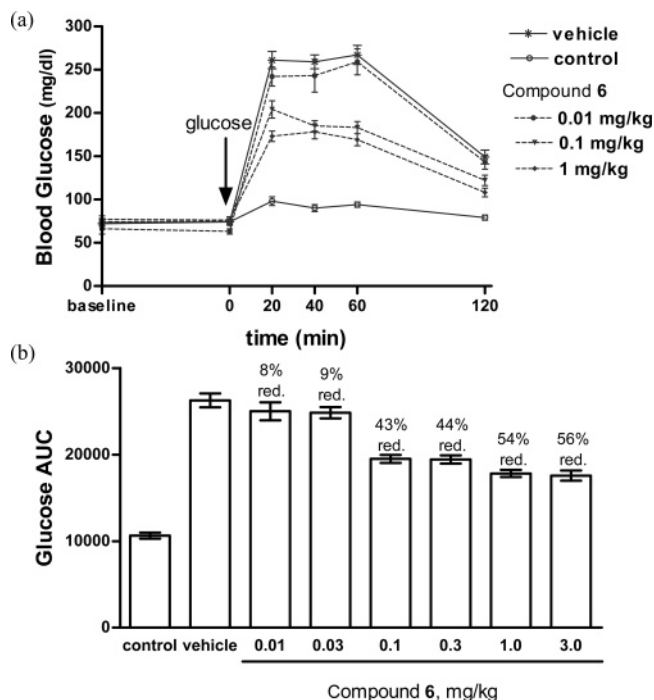


Figure 2. (a) Effects of compound **6** on glucose levels after an oral glucose tolerance test in lean C57BL/6N male mice. Compound **6** or water (vehicle) was administered 60 min prior to an oral dextrose challenge (5 g/kg). Control animals received water only. (b) The glucose AUC was determined from 0 to 120 min. Percent reduction values for each treatment were generated from the AUC data normalized to the water-challenged controls. Data are represented as mean \pm SEM ($n = 7$).

corresponds to 56% DPP-4 inhibition (from Figure 3), the calculated free fraction concentration of 11 nM correlates well with the measured murine DPP-4 potency ($IC_{50} = 6.0$ nM) of **6b**, thus resolving the discrepancy between the observed in vivo efficacy and the measured in vitro potency in the mouse.³¹ These results confirm the correlation between DPP-4 inhibition, increase in GLP-1 levels, and an improvement in glucose tolerance.

Blood glucose lowering was also demonstrated in diet-induced obese (DIO) mice, which are hyperglycemic, hyperinsulinemic, and show impaired glucose tolerance in response to a dextrose challenge consistent with insulin resistance observed in type 2 diabetes mellitus. Compared to vehicle, an 84% glucose reduction was observed at the 0.3 mg/kg oral dose of compound **6b** (Figure 4), resulting in near normalization of glucose excursion relative to lean controls.

Conclusions. A culmination of work with phenylalanine-derived DPP-4 inhibitors has led to the discovery of compound **6**, a potent DPP-4 inhibitor with a moderate serum shift that demonstrates excellent in vitro selectivity and in vivo efficacy. On the basis of its DPP-4 potency, selectivity, in vivo efficacy, pharmacokinetic profile, and low potential for metabolic activation, compound **6**, (2*S*,3*S*)-3-amino-4-(3,3-difluoropyrrolidin-1-yl)-*N,N*-dimethyl-4-oxo-2-(4-[1,2,4]triazolo[1,5-*a*]pyridin-6-ylphenyl)butanamide, was chosen for further evaluation as a potential treatment of type 2 diabetes mellitus.

Experimental Section

General. All commercial chemicals and solvents are reagent grade and were used without further purification unless otherwise specified. ¹H NMR spectra were recorded on a Varian InNova 500 MHz instrument in CDCl₃ or CD₃OD solutions. Low-resolution mass spectra (MS) were determined on a Micromass Platform

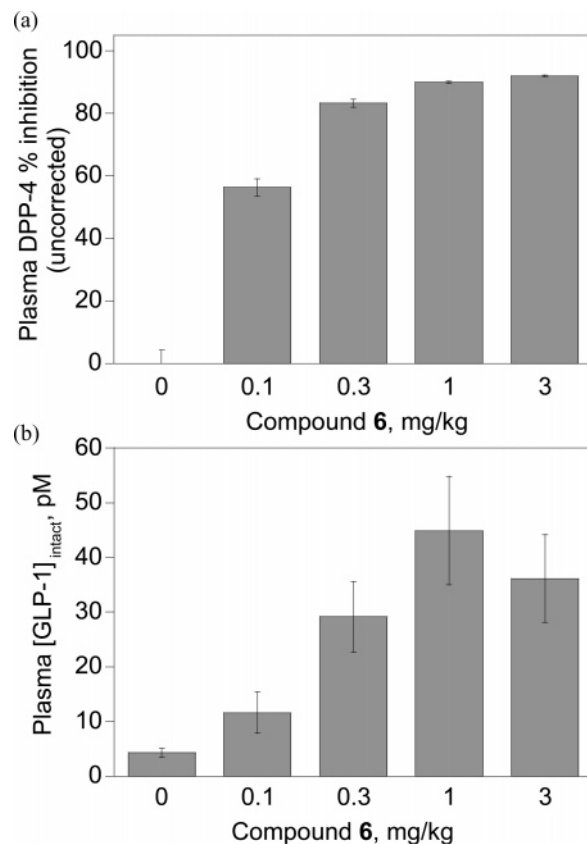


Figure 3. Effects of compound **6** on (a) DPP-4 inhibition and (b) GLP-1 levels after an oral glucose tolerance test in lean C57BL/6N male mice. Compound **6** was administered 60 min prior to an oral dextrose challenge (5 g/kg). Plasma samples were collected for analysis 10 min post-dextrose administration. Data are represented as mean \pm SEM ($n = 10$ –14/group).

Table 6. Plasma Protein Binding of Compound **6** in Different Species

mouse	rat	dog	monkey	human
96	91	64	54	82

Liquid Chromatography–Mass Spectrometer (LC–MS), using a Waters Xterra MSC18 3.5 μ m, 50 \times 3.0 mm column with a binary solvent system where solvent A = water, 0.06% trifluoroacetic acid (by volume) and solvent B = acetonitrile, 0.05% trifluoroacetic acid (by volume). The LC method used a flow rate = 1.0 mL/min with the following gradient: $t = 0$ min, 90% solvent A; $t = 3.75$ min., 2.0% solvent A; $t = 4.75$ min, 2% solvent A; $t = 4.76$ min, 90% solvent A; $t = 5.5$ min, 90% solvent A. High-resolution mass spectra were acquired from a Micromass Q-TOF quadrupole-time-of-flight mass spectrometer. All MS experiments were performed using electrospray ionization (EI) in positive ion mode. Leucine enkephalin was applied as a lock-mass reference for accurate mass analysis.

Purity analyses were performed using two distinct HPLC methods for each compound unless otherwise indicated. The above-described LC–MS HPLC method serves as a gross analysis of purity over a broad range, and all final compounds show a single peak (>95% purity) using this analytical method. To evaluate purity more accurately, a high-resolution HPLC method was used to evaluate each final product, and the final purity using these methods are noted with the analytical data. High-resolution HPLC purity analysis was achieved using the following two methods. Method A is composed of two 5 μ Intersil ODS-2 columns including a 4.6 \times 7.5 mm precolumn and a 4.6 \times 30 mm column, a flow rate = 2.0 mL/min, temperature = 37 $^{\circ}$ C, $\lambda = 210$ nm, and a mobile phase = 55:45 methanol/0.04 M potassium phosphate buffer with a final pH = 7.3. Method B utilized a 5 μ 4.6 \times 250 mm Intersil ODS-2 column at a flow rate = 0.7 mL/min, temperature = 37 $^{\circ}$ C, $\lambda =$

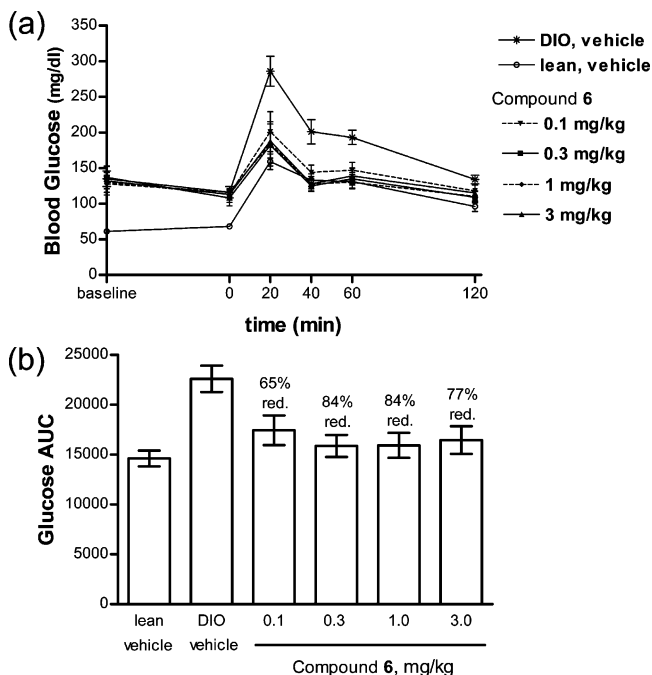


Figure 4. (a) Effects of compound **6** on glucose levels after an oral glucose tolerance test in diet-induced obese (DIO) C57BL/6N male mice versus lean mice. Compound **6** or water (vehicle) was administered 60 min prior to an oral dextrose challenge (5 g/kg). Control animals were lean and received vehicle followed by dextrose challenge. (b) The glucose AUC was determined from 0 to 120 min. Percent reduction values for each treatment were generated from the AUC data normalized to the lean controls. Data are represented as mean \pm SEM ($n = 7$).

210 nm, and a mobile phase = 55:45 methanol/0.04 M potassium phosphate buffer with a final pH = 7.3.

Potentiometric titration of products **4** and **6a** revealed that these compounds exist as mono-trifluoroacetic acid (TFA) salts with 0–54% excess TFA in the final forms. While amounts of excess TFA varied widely depending on the preparation of each individual batch, the ratios were typically closer to 1:1 parent/TFA when the final products were lyophilized to dryness. Consequently, final products **4**, **20**, **22**, **23**, **24**, and **27–32** likely exist as the corresponding mono-TFA salts. Final products with more basic heterocycles such as **21**, **25**, **26**, and **33** were not titrated. Potentiometric titration of hydrochloric acid salt **6b** revealed a ratio of 1.06:1 ratio of parent/HCl.

6-Bromo[1,2,4]triazolo[1,5-*a*]pyridine (8a). To a stirred solution of 2-amino-5-bromopyridine (25.0 g, 145 mmol) in *N,N*-dimethylformamide (60 mL) was added *N,N*-dimethylformamide dimethyl acetal (60.0 mL, 454 mmol). The reaction mixture was heated to 130 °C overnight. After cooling to room temperature, the volatiles were removed under reduced pressure to afford the desired product (*N'*-(5-bromopyridin-2-yl)-*N,N*-dimethylimidoforamide) as a brown oil.

To an ice-cooled, stirred solution of the above crude product in methanol (200 mL) and pyridine (23.0 mL, 290 mmol) was added hydroxylamine-*O*-sulfonic acid (22.6 g, 200 mmol). The reaction mixture was allowed to warm to room temperature and was stirred overnight. The volatiles were removed under reduced pressure, and the residue was partitioned between aqueous sodium bicarbonate solution and ethyl acetate. The aqueous layer was further extracted with ethyl acetate, and the combined organic layers were washed sequentially with water (100 mL) and saturated aqueous brine solution (100 mL), dried over magnesium sulfate, and concentrated in vacuo to yield **8a** as an orange/brown solid, which was used without further purification (18.8 g, 66% yield over two steps). LC/MS *m/e* 197.9/199.9 ($M + H$)⁺; ¹H NMR (500 MHz, CDCl₃) δ 8.77 (d, $J = 1.4$ Hz, 1H), 8.34 (s, 1H), 7.68 (d, $J = 9.4$ Hz, 1H), 7.60 (dd, $J = 9.4, 1.9$ Hz).

6-Bromo-5-methyl[1,2,4]triazolo[1,5-*a*]pyridine (8b). Starting with 6-amino-3-bromo-2-picoline, the same procedures were followed as in the synthesis of **8a**. For **8b**, LC/MS *m/e* 197.9/199.9 ($M + H$)⁺; ¹H NMR (500 MHz, CDCl₃) δ 8.65 (s, 1H), 8.34 (s, 1H), 7.45 (s, 1H), 2.70 (s, 3H).

6-Bromo-8-methyl[1,2,4]triazolo[1,5-*a*]pyridine (8c). Starting with 2-amino-5-bromo-3-picoline, the same procedures were followed as in the synthesis of **8a**. For **8c**, LC/MS *m/e* 212.0/214.0 ($M + H$)⁺; ¹H NMR (500 MHz, CDCl₃) δ 8.41 (s, 1H), 7.74 (d, $J = 9.4$ Hz, 1H), 7.65 (d, $J = 9.4$ Hz, 1H), 3.00 (s, 3H).

6-Bromo-8-methyl[1,2,4]triazolo[1,5-*a*]pyridine (8d). Starting with 2-amino-5-bromopyridine and dimethylacetamide dimethyl acetal, the same procedures were followed as in the synthesis of **8a**. For **8d**, LC/MS *m/e* 212.1/214.1 ($M + H$)⁺; ¹H NMR (500 MHz, CD₃OD) δ 8.96 (s, 1H), 7.75 (dd, $J = 9.4, 1.8$ Hz, 1H), 7.60 (d, $J = 9.6$ Hz, 1H), 2.53 (s, 3H).

2-Amino-4-iodopyridine (10). To a stirred solution of 4-iodo-picolinic acid hemi-hydroiodide hydrate (1.0 g, 3.0 mmol) in 6 mL of *tert*-butyl alcohol, 6 mL of toluene, and 1.4 mL of triethylamine was added diphenylphosphoryl azide (1.1 mL, 5.0 mmol) dropwise over 15 min. The resultant solution was then warmed to 65 °C and, after 1.5 h, the bath temperature was raised to 100 °C. After 12 h, the solution was cooled and concentrated under reduced pressure, and the residue was partitioned between ethyl acetate (100 mL) and water (60 mL). The ethyl acetate layer was washed sequentially with saturated aqueous sodium bicarbonate solution (100 mL) and saturated aqueous brine (100 mL), dried over magnesium sulfate, and concentrated to afford a brown solid. Purification by flash chromatography (silica gel; 5% ethyl acetate–hexanes eluant) afforded a pale yellow solid, which was triturated with hexanes to afford the Boc protected amine as a white solid (570 mg, 30% yield). MS 265.1 ($M + 1 - tBu$). To a solution of the above product (1.5 g, 4.7 mmol) in 10 mL of dichloromethane was added trifluoroacetic acid (5 mL). The resultant solution was stirred at room temperature for 1 h, and the volatiles were removed under reduced pressure. The residue was dissolved in water (50 mL), and the solution was neutralized by portionwise addition of sodium bicarbonate. The mixture was extracted with ethyl acetate, and the extract was washed with saturated aqueous brine, dried over magnesium sulfate and concentrated to afford an off-white solid, which was triturated with hexanes to afford 2-amino-4-iodopyridine **10** (1.0 g, 97% yield) as a white powder. LC/MS *m/e* 221.1 ($M + H$)⁺; ¹H NMR (500 MHz, CD₃OD) δ 7.59 (d, $J = 7.2$ Hz, 1H), 7.04 (s, 1H), 6.93 (d, $J = 7.2$ Hz, 1H).

7-Iodo[1,2,4]triazolo[1,5-*a*]pyridine (11). To a stirred solution of **10** (1.0 g, 4.5 mmol) in *N,N*-dimethylformamide (3.0 mL) was added *N,N*-dimethylformamide dimethyl acetal (1.6 mL, 11 mmol). The reaction mixture was heated to 130 °C in a sealed tube overnight. After cooling to room temperature, the volatiles were removed under reduced pressure to afford a red oil, which was dissolved in 8.0 mL of methanol and 0.74 mL of pyridine. The solution was cooled in an ice bath, and hydroxylamine-*O*-sulfonic acid (668 mg, 5.9 mmol) was added in one portion. The reaction mixture was allowed to warm to room temperature and was stirred overnight. The volatiles were removed under reduced pressure, and the residue was partitioned between saturated aqueous brine solution and ethyl acetate. The aqueous layer was further extracted with ethyl acetate, and the combined organic layers were washed with saturated aqueous brine solution (100 mL), dried over magnesium sulfate, and concentrated under reduced pressure to afford the crude product as an orange solid. Purification by flash chromatography (silica gel; 0 to 4% methanol/methylene chloride gradient) afforded pure **11** (363 mg, 33% over two steps) as a pale yellow solid. LC/MS *m/e* 246.1 ($M + H$)⁺; ¹H NMR (500 MHz, CD₃OD) δ 8.60 (d, $J = 9.2$ Hz, 1H), 8.39 (s, 1H), 8.26 (s, 1H), 7.52 (d, $J = 9.2$ Hz, 1H).

(2*S*,3*E*)-4-(4-Bromophenyl)but-3-en-2-ol (13). To 1.92 g (48 mmol) of sodium hydride (60% dispersion in mineral oil) in 100 mL of THF at 0 °C was added 8.1 g (42 mmol) of diethyl (2-oxopropyl)phosphonate, and the resultant mixture was stirred at 0 °C for 30 min. After the slurry became homogeneous, 7.4 g (38

mmol) of 4-bromobenzaldehyde was added to the mixture and the resulting solution was stirred for 2 h at 0 °C until TLC revealed complete disappearance of starting material. Next, the reaction mixture was diluted with 100 mL of water and the resultant mixture was extracted with three 200-mL portions of diethyl ether. The organic phases were then combined, washed with two 100 mL portions of 5% hydrochloric acid solution, two 100-mL portions of saturated aqueous sodium bicarbonate solution, two 100-mL portions of saturated aqueous brine, dried over magnesium sulfate, filtered, and evaporated in vacuo to yield the crude waxy solid. The crude material was then purified by flash chromatography on a Biotage system (silica gel, 0 to 15% ethyl acetate/hexanes gradient) to give 6.93 g (81% yield) of 3*E*-4-(4-bromophenyl)but-3-en-2-one as a pale yellow crystalline solid. LC/MS *m/e* 225.0/227.0 (M + H)⁺; ¹H NMR (500 MHz, CD₃OD) δ 7.54 (d, *J* = 8.5 Hz, 1H), 7.45 (d, *J* = 16.5 Hz, 1H), 7.42 (d, *J* = 9.5 Hz, 1H), 6.71 (d, *J* = 16.4 Hz, 1H), 2.39 (s, 3H).

To 121.5 g (540 mmol) of the above ketone dissolved in 2500 mL of toluene was added 75 mL (7.5 mmol, 1 M in toluene) of (*R*)-2-methyl-CBS-oxazaborolidine catalyst, and the resultant mixture was stirred with a mechanical stirrer at ambient temperature for 20 min. The mixture was cooled to -78 °C, and 92 mL (863 mmol) of catecholborane in 400 mL of toluene was added dropwise over 60 min. After the addition, the slurry was stirred at -78 °C for 60 min while slowly turning homogeneous. The solution was then stirred at -78 °C an additional 16 h (reaction time varies from 4 to 24 h) until TLC revealed complete disappearance of starting material. Next, the reaction mixture was warmed to room temperature and carefully quenched with 100 mL of water, diluted with 10 L of 1 N NaOH aqueous solution, and the resultant mixture was extracted (in an extractor) with 8000 mL of diethyl ether. The organic phases were then combined and washed with two 2500 mL portions of 1 N NaOH aqueous solution, 2000 mL of water, 2000 mL of 1 N aqueous hydrochloric acid, 1000 mL of saturated aqueous brine, dried over magnesium sulfate, filtered, and evaporated in vacuo to yield the crude yellow solid which was recrystallized slowly from hexane to give alcohol **13** (110 g, 90% yield) as pale yellow crystals. Analytical chiral HPLC (AD column, 2% ethanol/heptane) indicated that this product was 96% ee (*S* enantiomer is faster eluting). An additional recrystallization in cyclohexane afforded the *S* enantiomer **13** as colorless crystals in 98.2% ee (87.3 g, 71% overall yield). LC/MS *m/e* 209.0/211.0 (M - H₂O + 1)⁺; ¹H NMR (500 MHz, CD₃OD) δ 7.46 (d, *J* = 8.5 Hz, 2H), 7.26 (d, *J* = 8.5 Hz, 2H), 6.53 (d, *J* = 15.8 Hz, 1H), 6.28 (dd, *J* = 16.0, 6.2 Hz, 1H), 4.51 (m, 1H), 1.72 (s, 1H), 1.40 (d, *J* = 6.4 Hz, 3H).

(1*S*,2*E*)-3-(4-Bromophenyl)-1-methylprop-2-en-1-yl *N*-(*tert*-Butoxycarbonyl)glycinate (14**).** To 12.6 g (55 mmol) of alcohol **13** dissolved in anhydrous dichloromethane (300 mL) were added EDC (23 g, 120 mmol), HOBt (16 g, 120 mmol), *N*-(*tert*-butoxycarbonyl)glycine (21 g, 120 mmol), and *N,N'*-diisopropylethylamine (19 mL, 120 mmol). After 5 h, the mixture was concentrated and diluted with 200 mL of 10% aqueous hydrochloric acid. The resultant mixture was then extracted with three 300-mL portions of diethyl ether, and the organic phases were combined and washed sequentially with 5% hydrochloric acid, saturated aqueous sodium bicarbonate solution, and saturated aqueous brine (100 mL each). The organic phase was then dried over magnesium sulfate, filtered, and evaporated in vacuo to yield the crude material as a viscous oil. The crude material was purified by flash chromatography on a Biotage system (silica gel, 0 to 20% ethyl acetate/hexanes gradient) to give ester **14** (18.1 g, 86% yield) as a colorless crystalline solid. LC/MS *m/e* 328.1/330.1 (M - *t*Bu + 1)⁺; ¹H NMR (500 MHz, CD₃OD) δ 7.43 (d, *J* = 8.2 Hz, 2H), 7.23 (d, *J* = 8.4 Hz, 2H), 6.55 (d, *J* = 15.8 Hz, 1H), 16.16 (dd, *J* = 15.9, 6.7 Hz, 1H), 5.57 (m, 1H), 5.12 (s, 1H), 3.97–3.88 (m, 2H), 1.45 (s, 9H), 1.43 (d, *J* = 6.4 Hz, 2H).

(*βS*)-4-Bromo-*N*-(*tert*-butoxycarbonyl)- β -[(1*E*)-prop-1-en-1-yl]-L-phenylalanine (16**).** Ester **14** (18.1 g, 47 mmol) in anhydrous tetrahydrofuran (50 mL) was added via cannula to 105 mL (105 mmol, 1 M in tetrahydrofuran) of lithium hexamethyldisilazide

solution precooled to -78 °C. After stirring for 10 min at that temperature, 55 mL of zinc chloride solution (55 mmol, 1 M in diethyl ether) was added at -78 °C. The resultant mixture was stirred at -78 °C for 5 h and then allowed to warm slowly to room temperature over 3 h. After stirring an additional 2 h at room temperature, the mixture was quenched with water and 5% hydrochloric acid (100 mL each). The resultant mixture was then extracted with three 300-mL portions of ethyl acetate, and the organic phases were combined and washed sequentially with 5% hydrochloric acid, saturated aqueous sodium bicarbonate solution, and saturated aqueous brine (200 mL each). The organic phase was then dried over magnesium sulfate, filtered, and evaporated in vacuo to yield the crude acid **16** as a yellow foam. This crude material was dissolved in 500 mL of 1:1 diethyl ether/methanol and cooled to 0 °C. Trimethylsilyldiazomethane solution (75 mL, 150 mmol, 2 M in hexanes) was added in portions until a yellow color persisted. After warming to room temperature, the solution was stirred an additional 8 h, then concentrated in vacuo. The crude material was purified by flash chromatography on a Biotage system (silica gel, 0 to 15% ethyl acetate/hexanes gradient) to give the methyl ester **15** as a colorless oil (16.5 g, 88% yield). LC/MS *m/e* 298.0/300.0 (M - Boc + H)⁺; ¹H NMR (500 MHz, CDCl₃) δ 7.44 (d, *J* = 8.4 Hz, 2H), 7.08 (d, *J* = 8.5 Hz, 2H), 5.68–5.56 (m, 2H), 4.87 (d, *J* = 8.6 Hz, 1H), 4.60 (t, *J* = 8.0 Hz, 1H), 3.67 (s, 4H), 1.70 (d, *J* = 5.5 Hz, 3H), 1.39 (s, 9H).

To a solution of 25.0 g (62.8 mmol) of methyl ester **15** in 600 mL of tetrahydrofuran (THF) were added in succession 200 mL of methanol and 200 mL (200 mmol) of 1 N aqueous sodium hydroxide solution. The reaction mixture was stirred at ambient temperature for 3 h, and then the methanol and THF were removed under reduced pressure. To the aqueous mixture was added 250 mL of 1 N hydrochloric acid, and the mixture was extracted with ethyl acetate (3 \times 300 mL). The combined organic extracts were washed with brine (300 mL) then dried over sodium sulfate, filtered, and concentrated in vacuo to afford the carboxylic acid **16** (24.1 g, 100% yield) which was used without further purification. LC/MS *m/e* 384.1/386.1 (M + H)⁺; ¹H NMR (500 MHz, CDCl₃) δ 7.45 (d, *J* = 8.5 Hz, 2H), 7.12 (d, *J* = 8.5 Hz, 2H), 5.72–5.60 (m, 2H), 4.92 (d, *J* = 8.9 Hz, 1H), 4.64 (t, *J* = 7.8 Hz, 1H), 3.76 (t, *J* = 7.0 Hz, 1H), 1.71 (d, *J* = 5.7 Hz, 3H), 1.41 (s, 9H).

General Procedure for the Synthesis of Bromides 18a–c. Step A. Synthesis of 17a–c. To a solution of acid **16** and cyclic amine R₂NH (3-fluoroazetidene,¹³ pyrrolidine, or (*S*)-3-fluoropyrrolidine¹⁴) in DMF were added HOBt, *N,N*-diisopropylethylamine (DIPEA), and EDC. The solution was stirred at ambient temperature under nitrogen for 12–18 h, then ethyl acetate was added and the mixture was washed sequentially with saturated aqueous sodium bicarbonate solution, 1 N hydrochloric acid, and brine. Next, the solution was dried over sodium or magnesium sulfate, filtered, concentrated in vacuo, and purified by flash chromatography using a Biotage Horizon system (silica gel, 100% hexanes to 100% ethyl acetate gradient) to afford amides **17a–c**.

Step B. Synthesis of Dimethyl Amides (18a–c). A round-bottom flask with water and sodium periodate was stirred until homogeneous then potassium permanganate was added to the mixture. To this dark purple solution were added potassium carbonate powder and olefins **17a–c** in a *tert*-butyl alcohol solution. The reaction mixture was stirred at ambient temperature for 12–24 h, then treated with saturated aqueous sodium sulfite solution, acidified with 1 N aqueous hydrochloric acid, and extracted with ethyl acetate. The combined organic extracts were washed with brine, and the resultant clear solution was dried over sodium or magnesium sulfate, filtered, and concentrated in vacuo to afford the crude acids which were used without further purification.

To a solution of the above acids in DMF was added HOBt, DIPEA, 2 N dimethylamine (in THF), and EDC. The reaction mixture was then stirred at ambient temperature for 12–18 h. Ethyl acetate was then added and the mixture was washed with saturated aqueous sodium bicarbonate solution, 1 N aqueous hydrochloric acid, and brine, dried over sodium or magnesium sulfate, filtered and concentrated in vacuo. Purification by flash chromatography

using a Biotage Horizon system (silica gel, 1:1 ethyl acetate/hexanes to 100% ethyl acetate to 10% methanol/ethyl acetate gradient) afforded the products **18a–c**.

(2S,3S)-3-*N*-(*tert*-butoxycarbonyl)amino-2-(4-bromophenyl)-4-(3-fluoroazetid-1-yl)-*N,N*-dimethyl-4-oxobutanamide (18a). Starting from 3-fluoroazetid-1-yl¹² and acid **16**, the procedures above provided compound **18a**. LC/MS *m/e* 372.1/374.1 ($M - \text{Boc} + \text{H}^+$); ¹H NMR (500 MHz, CDCl₃) δ 7.47 (d, $J = 8.2$ Hz, 2H), 7.26–7.22 (m, 2H), 5.42–5.30 (br d, $J = 54.2$ Hz, 1H), 4.93–4.60 (m, 3H), 4.47–4.07 (m, 4H), 2.92–2.90 (m, 6H), 1.24 (s, 9H).

(2S,3S)-3-*N*-(*tert*-butoxycarbonyl)amino-2-(4-bromophenyl)-4-*N,N*-dimethyl-4-oxo-4-pyrrolidin-1-ylbutanamide (18b). Starting from pyrrolidine and acid **16**, the procedures above provided compound **18b**. LC/MS *m/e* 468.1/470.1 ($M + \text{H}^+$); ¹H NMR (500 MHz, CDCl₃) δ 7.48 (d, $J = 8.2$ Hz, 2H), 7.27 (d, $J = 8.4$ Hz, 2H), 5.14 (t, $J = 10.5$ Hz, 1H), 4.98 (d, $J = 10.5$ Hz, 1H), 4.23 (d, $J = 10.3$ Hz, 1H), 4.02–3.99 (m, 1H), 3.74–3.70 (m, 1H), 3.53–3.45 (m, 2H), 2.92 (s, 3H), 2.90 (s, 3H), 2.08–1.88 (m, 2H), 1.22 (s, 9H).

(2S,3S)-3-*N*-(*tert*-Butoxycarbonyl)amino-2-(4-bromophenyl)-4-[(3S)-3-fluoropyrrolidin-1-yl]-*N,N*-dimethyl-4-oxobutanamide (18c). Starting from (*S*)-3-fluoropyrrolidine¹³ and acid **16**, the procedures above provided compound **18c**. LC/MS *m/e* 486.2/488.2 ($M + \text{H}^+$); ¹H NMR (500 MHz, CDCl₃) δ 7.43 (d, $J = 7.5$ Hz, 2H), 7.29–7.24 (m, 2H), 5.34–4.85 (m, 3H), 4.36–4.09 (m, 2H), 3.89–3.45 (m, 3H), 2.88 (d, $J = 13.0$ Hz, 3H), 2.86 (s, 3H), 2.34–2.03 (m, 2H), 1.18 (s, 9H).

General Procedure for the Synthesis of Boronates 19a–c. To bromides **18a–c** in dimethyl sulfoxide (DMSO) was added bis-(pinacolato)diboron, [1,1'-bis(diphenylphosphino)ferrocene]dichloropalladium(II) (complex with dichloromethane (1:1)), and potassium acetate. Nitrogen was then bubbled through the mixture for 3 min, then the mixture was stirred at 80 °C under nitrogen for 4–12 h. The mixture was cooled to ambient temperature, filtered through a silica gel pad, and rinsed with excess ethyl acetate. The solution was washed with two portions of brine, dried over sodium or magnesium sulfate, filtered, and concentrated in vacuo. Purification by flash chromatography on a Biotage Horizon system (silica gel, 40% ethyl acetate/hexanes to 100% ethyl acetate to 20% methanol/ethyl acetate gradient) afforded the boronates **19a–c** as dark yellow/brown foamy solids.

General Procedure for the Synthesis of Compounds 20–33.
Step A. Suzuki Coupling of Boronates 18a–c. To boronates **19a–c** in ethanol/toluene (1:1) were added ArX (5-bromo-1-methylpyridin-2(1*H*)-one,³² 6-iodoimidazo[1,2-*a*]pyridine, 6-bromo-[1,2,4]triazolo[4,3-*a*]pyridine,³³ **8a–d**, **11**, 5-chloropyrazolo[1,5-*a*]pyrimidine,³⁴ or 6-chloroimidazo[1,2-*b*]pyridazine³⁵), [1,1'-bis(diphenylphosphino)ferrocene]dichloro-palladium(II) (complex with dichloromethane, 1:1), and 2 N aqueous sodium carbonate solution. The reaction mixture was stirred at 90 °C under nitrogen for 8–14 h. After cooling to ambient temperature, ethyl acetate was added to the mixture and the organic phase was washed sequentially with 0.5 N aqueous sodium bicarbonate solution and brine, dried over sodium or magnesium sulfate, filtered, and concentrated in vacuo. The crude material was purified by reverse phase HPLC (YMC Pro-C18 column, gradient elution, 10 to 90% acetonitrile/water with 0.1% TFA) to afford the pure coupled products.

Step B. General Procedure for *tert*-Butyloxycarbonyl (Boc) Deprotection. The above coupled products were dissolved in a 1:1 mixture of dichloromethane and TFA, stirred for 30–90 min at room temperature, then concentrated in vacuo. Purification by reverse phase HPLC (YMC Pro-C18 column, gradient elution, 10 to 90% acetonitrile/water with 0.1% TFA) then afforded the pure final products **20–33**.

(2S,3S)-3-Amino-4-[(3S)-3-fluoropyrrolidin-1-yl]-*N,N*-dimethyl-2-[4-(1-methyl-6-oxo-1,6-dihydropyridin-3-yl)phenyl]-4-oxobutanamide, TFA Salt (20). Starting from bromide **18c** and 5-bromo-1-methylpyridin-2(1*H*)-one,³² the procedures summarized above provided compound **20**. 100% purity by HPLC (Method B, $t_r = 4.85$ min); LC/MS *m/e* 415.6 ($M + \text{H}^+$); HRMS (ES^+) calcd

for C₂₂H₂₇FN₄O₃ ($M + \text{H}^+$) *m/e* 415.2145, found *m/e* 415.2150. ¹H NMR (500 MHz, CD₃OD) δ 8.03 (d, $J = 2.6$ Hz, 1H), 7.91 (dd, $J = 9.4, 2.8$ Hz), 7.66 (d, $J = 8$ Hz), 7.48 (m, 1H), 6.66 (d, $J = 9.3$ Hz, 1H), 5.40 (m, 1H), 4.66 (dd, $J = 24.5, 8$ Hz, 1H), 4.54 (dd, $J = 14.2, 8$ Hz, 1H), 4.38 (dt, $J = 31.8, 11.5, 9.0$ Hz, 1 H), 3.85 (m, 2H), 3.66 (s, 3H), 3.55, (m, 1H), 2.93 (dd, $J = 12.3, 4.7$ Hz, 6H), 2.25 (m, 2H).

(2S,3S)-3-Amino-4-[(3S)-3-fluoropyrrolidin-1-yl]-2-(4-imidazo[1,2-*a*]pyridin-6-ylphenyl)-*N,N*-dimethyl-4-oxobutanamide, TFA Salt (21). Starting from bromide **18c** and 6-iodoimidazo[1,2-*a*]pyridine, the procedures summarized above provided compound **21**. 98.8% purity by HPLC (Method B, $t_r = 5.90$ min); LC/MS *m/e* 424.2 ($M + \text{H}^+$); HRMS (ES^+) calcd for C₂₃H₂₆FN₅O₂ ($M + \text{H}^+$) *m/e* 424.2149, found *m/e* 424.2169. ¹H NMR (500 MHz, CD₃OD) δ 9.14 (s, 1H), 8.29 (d, $J = 1.4$ Hz, 1H), 8.28 (d, $J = 2.1$ Hz, 1H), 8.09 (d, $J = 2.1$ Hz, 1H), 8.04 (d, $J = 9.4$ Hz, 1H), 7.85 (d, $J = 8.2$ Hz, 2H), 7.62 (d, $J = 8.2$ Hz, 2H), 5.32 (dd, $J = 52.7, 33.7$ Hz, 1H), 4.72 (dd, $J = 25.6, 8.4$ Hz, 1H), 4.62 (dd, $J = 13.6, 8.4$ Hz, 1H), 4.44–4.33 (m, 1H), 3.94–3.79 (m, 2H), 3.67–3.49 (m, 1H), 2.97 (d, $J = 7.1$ Hz, 3H), 2.92 (d, $J = 3.2$ Hz, 3H), 2.42–2.16 (m, 2H).

(2S,3S)-3-Amino-4-[(3S)-3-fluoropyrrolidin-1-yl]-*N,N*-dimethyl-4-oxo-2-(4-[1,2,4]triazolo[4,3-*a*]pyridin-6-ylphenyl)butanamide, TFA Salt (22). Starting from bromide **18c** and 6-bromo-[1,2,4]triazolo[4,3-*a*]pyridine,³³ the procedures summarized above provided compound **22**. 99.2% purity by HPLC (Method B, $t_r = 4.35$ min); LC/MS *m/e* 425.2 ($M + \text{H}^+$); HRMS (ES^+) calcd for C₂₂H₂₆FN₆O₂ ($M + \text{H}^+$) *m/e* 425.2101, found *m/e* 425.2114. ¹H NMR (500 MHz, CD₃OD) δ 9.45 (s, 1H), 9.06 (s, 1H), 8.26 (d, $J = 9.2$ Hz, 1H), 8.08 (d, $J = 9.2$ Hz, 1H), 7.83 (d, $J = 8.0$ Hz, 2H), 7.62 (d, $J = 8.0$ Hz, 2H), 5.39 (dd, $J = 53.5, 34.6$ Hz, 1H), 4.73 (dd, $J = 26.3, 8.3$ Hz, 1H), 4.62 (dd, $J = 13.2, 8.3$ Hz, 1H), 4.41–4.34 (m, 1H), 3.96–3.80 (m, 2H), 3.67–3.48 (m, 1H), 2.97 (d, $J = 7.8$ Hz, 3H), 2.92 (d, $J = 2.3$ Hz, 3H), 2.41–2.08 (m, 2H).

(2S,3S)-3-Amino-4-[(3S)-3-fluoropyrrolidin-1-yl]-*N,N*-dimethyl-4-oxo-2-(4-[1,2,4]triazolo[1,5-*a*]pyridin-6-ylphenyl)butanamide, TFA Salt (23). Starting from bromide **18c** and intermediate **8a**, the procedures summarized above provided compound **23**. 97.7% purity by HPLC (Method B, $t_r = 5.86$ min); LC/MS *m/e* 425.3 ($M + \text{H}^+$); HRMS (ES^+) calcd for C₂₂H₂₆FN₆O₂ ($M + \text{H}^+$) *m/e* 425.2101, found *m/e* 425.2106. ¹H NMR (500 MHz, CD₃OD) δ 9.10 (s, 1H), 8.48 (s, 1H), 8.03 (dt, $J = 9.2, 2.1$ Hz, 1H), 7.88 (d, $J = 9.3$ Hz, 1H), 7.82 (dd, $J = 8.2, 2.7$ Hz, 2H), 7.57 (dd, $J = 8.5, 3.7$ Hz, 2H), 5.40 (dd, $J = 53.2, 37.8$ Hz, 1H), 4.71 (dd, $J = 24.3, 8.3$ Hz, 1H), 4.61 (dd, $J = 14.4, 8.2$ Hz, 1H), 4.44–4.34 (m, 1H), 3.93–3.79 (m, 2H), 3.67–3.50 (m, 1H), 2.97 (d, $J = 5.3$ Hz, 3H), 2.93 (d, $J = 3.4$ Hz, 3H), 2.45–2.15 (m, 2H).

(2S,3S)-3-Amino-4-[(3S)-3-fluoropyrrolidin-1-yl]-*N,N*-dimethyl-4-oxo-2-(4-[1,2,4]triazolo[1,5-*a*]pyridin-7-ylphenyl)butanamide, TFA Salt (24). Starting from bromide **18c** and intermediate **11**, the procedures summarized above provided compound **24**. 99.7% purity by HPLC (Method B, $t_r = 5.86$ min); LC/MS *m/e* 425.3 ($M + \text{H}^+$); HRMS (ES^+) calcd for C₂₂H₂₆FN₆O₂ ($M + \text{H}^+$) *m/e* 425.2101, found *m/e* 425.2117. ¹H NMR (500 MHz, CD₃OD) δ 8.92 (d, $J = 7.3$ Hz, 1H), 8.57 (s, 1H), 8.08 (s, 1H), 7.92 (d, $J = 8.2$ Hz, 2H), 7.63 (d, $J = 7.3$ Hz, 1H), 7.60 (dd, $J = 8.4, 2.0$ Hz, 2H), 5.40 (dd, $J = 53.4, 35.1$ Hz, 1H), 4.75–4.33 (m, 3H), 3.93–3.31 (m, 3H), 2.97 (d, $J = 6.2$ Hz, 3H), 2.93 (d, $J = 3.6$ Hz, 3H), 2.45–2.07 (m, 2H).

(2S,3S)-3-Amino-4-[(3S)-3-fluoropyrrolidin-1-yl]-*N,N*-dimethyl-4-oxo-2-(4-pyrazolo[1,5-*a*]pyrimidin-5-ylphenyl)butanamide, TFA Salt (25). Starting from bromide **18c** and 5-chloropyrazolo[1,5-*a*]pyrimidine,³⁴ the procedures summarized above provided compound **25**. 98.8% purity by HPLC (Method B, $t_r = 7.13$ min); LC/MS *m/e* 425.3 ($M + \text{H}^+$); HRMS (ES^+) calcd for C₂₂H₂₆FN₆O₂ ($M + \text{H}^+$) *m/e* 425.2101, found *m/e* 425.2114. ¹H NMR (500 MHz, CD₃OD) δ 8.91 (d, $J = 7.6$ Hz, 1H), 8.21–8.18 (m, 3H), 7.58 (d, $J = 7.7$ Hz, 2H), 7.51 (d, $J = 7.3$ Hz, 1H), 6.72 (d, $J = 2.1$ Hz, 1H), 5.41 (dd, $J = 52.2, 34.1$ Hz, 1H), 4.74 (dd, $J = 26.8, 8.0$ Hz, 1H), 4.63 (dd, $J = 16.0, 8.1$ Hz, 1H), 4.45–4.34 (m, 1H), 3.97–3.51 (m, 3H), 2.97–2.93 (m, 6H), 2.43–2.30 (m, 2H).

(2S,3S)-3-Amino-4-[(3S)-3-fluoropyrrolidin-1-yl]-2-(4-imidazo[1,2-*b*]pyridazin-6-ylphenyl)-*N,N*-dimethyl-4-oxobutanamide, TFA Salt (26). Starting from bromide **18c** and 6-chloroimidazo[1,2-*b*]pyridazine,³⁵ the procedures summarized above provided compound **26**. LC/MS *m/e* 425.4 (M + H)⁺; HRMS (ES⁺) calcd for C₂₂H₂₆FN₆O₂ (M + H)⁺ *m/e* 425.2101, found *m/e* 425.2090. ¹H NMR (500 MHz, CD₃OD) δ 8.46 (s, 1H), 8.38 (d, *J* = 9.8 Hz, 1H), 8.24–8.20 (m, 3H), 8.11 (s, 1H), 7.65 (d, *J* = 8.0 Hz, 1H), 5.41 (dd, *J* = 52.7, 34.4, 1H), 4.73 (dd, *J* = 24.7, 8.2 Hz, 1H), 4.64 (dd, *J* = 14.1, 8.2 Hz, 1H), 4.45–4.34 (m, 1H), 3.93–3.79 (m, 2H), 3.68–3.51 (m, 1H), 3.34–3.32 (m, 3H), 2.98–2.93 (m, 3H), 2.46–2.04 (m, 2H).

(2S,3S)-3-Amino-4-[(3S)-3-fluoropyrrolidin-1-yl]-*N,N*-dimethyl-2-[4-(2-methyl[1,2,4]triazolo[1,5-*a*]pyridin-6-yl)phenyl]-4-oxobutanamide, TFA Salt (27). Starting from bromide **18c** and intermediate **8d**, the procedures summarized above provided compound **27**. 99.6% purity by HPLC (Method A, *t_r* = 0.376 min); LC/MS *m/e* 439.2 (M + H)⁺; HRMS (ES⁺) calcd for C₂₃H₂₈FN₆O₂ (M + H)⁺ *m/e* 439.2252, found *m/e* 439.2257. ¹H NMR (500 MHz, CD₃OD) δ 9.04 (d, *J* = 0.7 Hz, 1H), 8.07 (dt, *J* = 9.2, 1.6 Hz, 1H), 7.84–7.81 (m, 3H), 7.58–7.55 (m, 2H), 5.40 (dd, *J* = 52.6, 34.5, 1H), 4.70 (dd, *J* = 24.5, 8.2 Hz, 1H), 4.59 (dd, *J* = 14.4, 8.0 Hz, 1H), 4.44–4.33 (m, 1H), 3.92–3.78 (m, 2H), 3.67–3.50 (m, 1H), 2.96 (d, *J* = 5.2 Hz, 3H), 2.93 (d, *J* = 5.1 Hz, 3H), 2.61 (s, 3H), 2.43–2.06 (m, 2H).

(2S,3S)-3-Amino-4-[(3S)-3-fluoropyrrolidin-1-yl]-*N,N*-dimethyl-2-[4-(5-methyl[1,2,4]triazolo[1,5-*a*]pyridin-6-yl)phenyl]-4-oxobutanamide, TFA Salt (28). Starting from bromide **18c** and intermediate **8b**, the procedures summarized above provided compound **28**. 99.8% purity by HPLC (Method B, *t_r* = 7.04 min); LC/MS *m/e* 439.3 (M + H)⁺; HRMS (ES⁺) calcd for C₂₃H₂₈FN₆O₂ (M + H)⁺ *m/e* 439.2258, found *m/e* 439.2266. ¹H NMR (500 MHz, CD₃OD) δ 8.58 (d, *J* = 1.4 Hz, 1H), 7.80 (d, *J* = 8.9 Hz, 1H), 7.74 (d, 9.1 Hz, 1H), 7.59 (d, *J* = 1.8 Hz, 4H), 5.42 (dd, *J* = 52.6, 39.9 Hz, 1H), 4.73 (dd, *J* = 24.4, 8.1 Hz, 1H), 4.63 (dd, *J* = 13.9, 8.1 Hz, 1H), 4.46–4.35 (m, 1H), 3.95–3.81 (m, 2H), 3.69–3.52 (m, 1H), 3.01 (d, *J* = 5.3 Hz, 3H), 2.96 (d, 3.9 Hz, 3H), 2.83 (s, 3H), 2.44–2.28 (m, 2 H).

(2S,3S)-3-Amino-4-[(3S)-3-fluoropyrrolidin-1-yl]-*N,N*-dimethyl-2-[4-(8-methyl[1,2,4]triazolo[1,5-*a*]pyridin-6-yl)phenyl]-4-oxobutanamide, TFA Salt (29). Starting from bromide **18c** and intermediate **8c**, the procedures summarized above provided compound **29**. 98.5% purity by HPLC (Method A, *t_r* = 0.441 min); LC/MS *m/e* 439.2 (M + H)⁺; HRMS (ES⁺) calcd for C₂₃H₂₈FN₆O₂ (M + H)⁺ *m/e* 439.2252, found *m/e* 439.2260. ¹H NMR (500 MHz, CD₃OD) δ 8.97 (s, 1H), 8.49 (s, 1H), 7.87–7.84 (m, 4H), 7.59–7.56 (m, 3H), 5.42 (dd, *J* = 52.6, 34.6 Hz, 1H), 4.71 (dd, *J* = 24.2, 8.2 Hz, 1H), 4.60 (dd, *J* = 14.6, 8.0 Hz, 1H) 4.42–4.35 (m, 1H), 3.94–3.80 (m, 2H), 3.69–3.55 (m, 1H), 2.98 (d, *J* = 5 Hz, 3H), 2.95 (d, *J* = 4.4 Hz, 3H), 2.72 (s, 3H), 2.44–2.31 (m, 2H).

(2S,3S)-3-Amino-4-(3-fluoroazetidin-1-yl)-*N,N*-dimethyl-4-oxo-2-[4-[1,2,4]triazolo[1,5-*a*]pyridin-6-ylphenyl]butanamide, TFA Salt (30). Starting from bromide **18a** and intermediate **8a**, the procedures summarized above provided compound **30**. 100% purity by HPLC (Method B, *t_r* = 5.63 min); LC/MS *m/e* 411.2 (M + H)⁺; HRMS (ES⁺) calcd for C₂₁H₂₄FN₆O₂ (M + H)⁺ *m/e* 411.1939, found *m/e* 411.1954. ¹H NMR (500 MHz, CD₃OD) δ 9.13 (s, 1H), 8.50 (s, 1H) 8.07 (dd, *J* = 9.3, 1.8 Hz, 1H), 7.91 (dd, *J* = 9.3, 0.8 Hz, 1H), 7.86 (d, *J* = 8.2 Hz, 2H), 7.60–7.58 (m, 2H), 5.47 (bd, *J* = 57 Hz, 1H), 5.30–4.95 (m, 1H), 4.81–4.74 (m, 1H), 4.57–4.37 (m, 3H), 4.21–4.14 (m, 1H), 2.98 (d, *J* = 5.2 Hz, 3H), 2.96 (d, *J* = 6.9 Hz, 3H).

(2S,3S)-3-Amino-*N,N*-dimethyl-4-oxo-4-pyrrolidin-1-yl-2-[4-[1,2,4]triazolo[1,5-*a*]pyridin-6-ylphenyl]butanamide, TFA Salt (31). Starting from bromide **18b** and intermediate **8a**, the procedures summarized above provided compound **31**. 96.8% purity by HPLC (Method A, *t_r* = 0.423 min); LC/MS *m/e* 407.3 (M + H)⁺; HRMS (ES⁺) calcd for C₂₂H₂₇N₆O₂ (M + H)⁺ *m/e* 407.2190, found *m/e* 407.2196. ¹H NMR (500 MHz, CD₃OD) δ 9.10 (s, 1H), 8.50 (s, 1H), 8.05 (d, *J* = 9.4 Hz, 1H), 7.89 (d, *J* = 9.4 Hz, 1H), 7.82 (d, *J* = 8.3 Hz, 2H), 7.56 (d, *J* = 8.1 Hz, 2H), 4.71 (d, *J* = 7.8 Hz,

1H), 4.61 (d, *J* = 7.7 Hz, 1 H), 4.03–3.98 (m, 1H), 3.76–3.71 (m, 1H), 3.56–3.46 (m, 2H), 2.97 (s, 3H), 2.94 (s, 3H), 2.15–1.96 (m, 4H).

(2S,3S)-3-Amino-4-(3,3-difluoropyrrolidin-1-yl)-*N,N*-dimethyl-4-oxo-2-[4-[1,2,4]triazolo[1,5-*a*]pyridin-7-ylphenyl]butanamide, TFA Salt (32). Starting from bromide **18d** and intermediate **11**, the procedures summarized above provided compound **32**. 95.2% purity by HPLC (Method B, *t_r* = 6.51 min); LC/MS *m/e* 443.2 (M + H)⁺; HRMS (ES⁺) calcd for C₂₂H₂₅F₂N₆O₂ (M + H)⁺ *m/e* 443.2002, found *m/e* 443.2031. ¹H NMR (500 MHz, CD₃OD) δ 9.02 (d, *J* = 7.0 Hz, 1H), 8.80 (s, 1H), 8.19 (s, 1H), 7.98 (d, *J* = 8.3 Hz, 2H), 7.78 (d, *J* = 6.9 Hz, 1H), 7.63 (dd, *J* = 8.1, 2.0 Hz, 2H), 4.78–3.72 (series of m, 6H), 2.96 (s, 3H), 2.94 (d, *J* = 1.5 Hz, 3H), 2.66–2.45 (m, 2H).

(2S,3S)-3-Amino-4-(3,3-difluoropyrrolidin-1-yl)-*N,N*-dimethyl-4-oxo-2-(4-pyrazolo[1,5-*a*]pyrimidin-5-ylphenyl)butanamide, TFA Salt (33). Starting from bromide **18d** and 6-chloroimidazo[1,2-*b*]pyridazine,³⁵ the procedures summarized above provided compound **33**. High-resolution HPLC purity was not evaluated, but the sample was >95% pure by LC/MS HPLC method. LC/MS *m/e* 443.3 (M + H)⁺. ¹H NMR (500 MHz, CD₃OD) δ 8.95 (d, *J* = 7.4 Hz, 1H), 8.26 (d, *J* = 8.2 Hz, 2H), 8.19 (d, *J* = 2.3 Hz, 1H), 7.59 (d, *J* = 8.3 Hz, 2H), 7.57 (d, *J* = 7.3 Hz, 1H), 6.73 (t, *J* = 1.7 Hz, 1H), 4.75 (d, *J* = 8.3 Hz, 1H), 4.64–4.57 (m, 2H), 4.55–3.73 (series of m, 4H), 3.32–3.31 (m, 3H), 2.94 (d, *J* = 10.7 Hz, 3H), 2.67–2.43 (m, 2H).

(2S,3S,4E)-3-(4-Bromophenyl)-1-(3,3-difluoropyrrolidin-1-yl)-1-oxohex-4-en-2-*N*-(*tert*-butoxycarbonyl)amine (17d). Acid **16** (15 g, 39 mmol) was mixed with 11.2 g (78 mmol) of 3,3-difluoropyrrolidine,¹³ 10.5 g (78 mmol) of HOBt, 13.7 mL (78 mmol) of *N,N*-diisopropylethylamine, and 200 mL of DMF. Next, 15 g (78 mmol) of EDC was added, and the solution was stirred at ambient temperature under nitrogen for 12 h. Ethyl acetate (1.0 L) was added, and the mixture was washed with 0.5 N aqueous sodium bicarbonate solution (3 \times 400 mL), 1 N hydrochloric acid (2 \times 400 mL), and brine (400 mL), dried over sodium sulfate, filtered, and concentrated in vacuo to afford **17d** (17.7 g, 96% yield), which was sufficiently pure for use in subsequent steps. LC/MS *m/e* 375.1 (M – Boc + H)⁺; ¹H NMR (500 MHz, CDCl₃) δ 7.48 (d, *J* = 8.4 Hz, 2H), 7.15 (d, *J* = 8.3 Hz, 2H), 5.72–5.59 (m, 2H), 5.10–5.08 (m, 1H), 4.72–4.53 (m, 1H), 4.03–3.32 (m, 5H), 2.41–2.14 (m, 2H), 1.71 (d, *J* = 6.2 Hz, 3H), 1.37 (s, 9H).

(2S,3S)-*N*-(*tert*-Butoxycarbonyl)amino-2-(4-bromophenyl)-4-(3,3-difluoropyrrolidin-1-yl)-*N,N*-dimethyl-4-oxobutanamide (18d). A round-bottom flask was charged with 1.5 L of water, and 80 g (374 mmol) of sodium periodate was added. The mixture was stirred until homogeneous then 1.2 g (7.5 mmol) of potassium permanganate was added to the mixture. To this dark purple solution were added 5.7 g (41.1 mmol) of potassium carbonate powder (~325 mesh) and 17.7 g (37.4 mmol) of **17d** as a 500 mL *tert*-butyl alcohol solution. The reaction mixture was stirred at ambient temperature for 24 h, then treated with 50 mL of saturated aqueous sodium sulfite solution, acidified with 1 N aqueous hydrochloric acid (400 mL), and extracted with ethyl acetate (3 \times 400 mL). The combined organic extracts were washed with brine (3 \times 400 mL), and the resultant clear solution was dried over sodium sulfate, filtered, and concentrated in vacuo to afford the crude acid (20.38 g, 100%) as a colorless crystalline solid which was used without further purification. LC/MS *m/e* 377.0/379.0 (M + H)⁺; ¹H NMR (500 MHz, CD₃OD) δ 7.48–7.46 (m, 2H), 7.26–7.22 (m, 2H), 7.12 (br s, 1H), 5.35 (dd, *J* = 21.0, 10.4 Hz, 1H), 5.12–4.94 (m, 1H), 4.21–4.00 (m, 3H), 3.91–3.65 (m, 2H), 2.50–2.33 (m, 2H), 1.24 (d, *J* = 4.6 Hz, 9H).

The above acid (20.38 g, 37.4 mmol) was mixed with 10.1 g (74.8 mmol) of HOBt and 300 mL of DMF. Next, 13 mL (74.8 mmol) of *N,N*-diisopropylethylamine, 37.4 mL (74.8 mmol) of 2 N dimethylamine in THF, and 14.3 g (74.8 mmol) of EDC were then added sequentially to the solution. The reaction mixture was then stirred at ambient temperature for 12 h. Ethyl acetate (1.2 L) was then added, and the mixture was washed with 0.5 N aqueous sodium bicarbonate solution (3 \times 400 mL), 1 N aqueous hydro-

chloric acid (2 × 300 mL), and brine (400 mL), dried over sodium sulfate, filtered, and concentrated in vacuo. Purification by flash chromatography using a Biotage Horizon system (silica gel, 1:1 ethyl acetate/hexanes to 100% ethyl acetate to 10% methanol/ethyl acetate gradient) afforded dimethyl amide **18d** as a pale yellow foamy solid (11.53 g, 59% yield). LC/MS *m/e* 448.2/450.2 (M + H)⁺; ¹H NMR (500 MHz, CDCl₃) δ 7.47 (d, *J* = 8.3 Hz, 2H), 7.26–7.24 (m, 2H), 5.16–4.94 (m, 1H), 4.79–4.74 (t, *J* = 10.8 Hz, 1H), 4.36–4.13 (m, 2H), 3.97–3.64 (m, 3H), 2.91 (s, 3H), 2.90 (s, 3H), 2.53–2.36 (m, 2H), 1.22 (d, *J* = 3.3 Hz, 9H).

(2S,3S)-3-*N*-(*tert*-Butoxycarbonyl)amino-4-(3,3-difluoropyrrolidin-1-yl)-*N,N*-dimethyl-4-oxo-2-[4-(4,4,5,5-tetramethyl-1,3,2-dioxaborolan-2-yl)phenyl]butanamide (19d). To 11.5 g (22.8 mmol) of **18d** were added 11.5 (45.6 mmol) of bis(pinacolato)diboron, 3.7 g (4.6 mmol) of [1,1'-bis(diphenylphosphino)ferrocene]dichloropalladium(II) (complex with dichloromethane (1:1)), 11.2 g (114 mmol) of potassium acetate, and 70 mL of dimethyl sulfoxide (DMSO). Nitrogen was then bubbled through the mixture for 3 min, then the mixture was stirred at 80 °C under nitrogen for 4 h. The mixture was cooled to ambient temperature, then filtered through a silica gel pad and rinsed with excess ethyl acetate. The solution was washed with two portions of brine, dried over sodium sulfate, filtered, and concentrated in vacuo. Purification by flash chromatography on a Biotage Horizon system (silica gel, 40% ethyl acetate/hexanes to 100% ethyl acetate to 20% methanol/ethyl acetate gradient) afforded **19d** as a yellow foamy solid (10.5 g, 84%). LC/MS *m/e* 552.6 (M + H)⁺; ¹H NMR (500 MHz, CDCl₃) δ 7.71 (d, *J* = 7.7 Hz, 2H), 7.37 (dd, *J* = 7.9, 1.7 Hz, 2H), 5.02 (t, *J* = 10.4 Hz, 1H), 4.38 (d, *J* = 10.6 Hz, 1H), 4.19–3.58 (m, 4H), 2.95 (s, 3H), 2.90 (s, 3H), 1.35 (s, 12H), 1.18 (d, *J* = 5.5 Hz, 9H).

(2S,3S)-3-Amino-4-(3,3-difluoropyrrolidin-1-yl)-*N,N*-dimethyl-4-oxo-2-(4-[1,2,4]triazolo[1,5-*a*]pyridin-6-ylphenyl)butanamide, TFA Salt (6a). To 9.27 g (16.8 mmol) of **19d** in 200 mL of ethanol/toluene (1:1) were added 6.7 g (33.6 mmol) of 6-bromo-[1,2,4]triazolo[1,5-*a*]pyridine **8a**, 2.9 g (3.6 mmol) of [1,1'-bis(diphenylphosphino)ferrocene]dichloropalladium(II) (complex with dichloromethane, 1:1), and 42 mL (84 mmol) of 2 N aqueous sodium carbonate solution. The reaction mixture was stirred at 90 °C under nitrogen for 12 h. After cooling to ambient temperature, 600 mL of ethyl acetate was added to the mixture and the organic phase was washed sequentially with 0.5 N aqueous sodium bicarbonate solution and brine, dried over sodium sulfate, filtered, and concentrated in vacuo. The crude material was purified by reverse phase HPLC on a Kiloprep 100 G system (Kromasil C₈ 16 micron, isocratic elution, 40% acetonitrile/water with 0.1% TFA) to afford the coupled product as a colorless solid (6.9 g, 76% yield). LC/MS *m/e* 543.27 (M + H)⁺; ¹H NMR (500 MHz, CD₃OD) δ 9.05 (s, 1H), 8.46 (s, 1H), 8.01 (d, *J* = 9.1 Hz, 1H), 7.87 (d, *J* = 9.1 Hz, 1H), 7.73 (d, *J* = 7.5 Hz, 2H), 7.55 (d, *J* = 7.5 Hz, 2H), 5.03 (dd, *J* = 76.7, 10.3 Hz, 1H), 4.46 (d, *J* = 10.5 Hz, 1H), 4.23–3.61 (m, 4H), 3.02 (s, 3H), 2.92 (s, 3H), 2.58–2.42 (m, 2H), 1.20 (d, *J* = 5.0 Hz, 9H).

The coupled product was then dissolved in a 1:1 mixture of dichloromethane and TFA, stirred for 30 min at room temperature, then concentrated in vacuo. The product was purified by reverse phase HPLC on a Kiloprep 100 G system (Kromasil C₈ 16 micron, gradient elution, 0% to 65% acetonitrile/water with 0.1% TFA) to afford the product **6a** as a colorless crystalline TFA salt (3.7 g, 60% yield). 100% purity by HPLC (Method A, *t_r* = 0.462 min); LC/MS *m/e* 443.5 (M + H)⁺; HRMS (ES⁺) calcd for C₂₂H₂₅F₂N₆O₂ (M + H)⁺ *m/e* 443.2007, found *m/e* 443.2027. ¹H NMR (500 MHz, CD₃OD) δ 9.12 (s, 1H), 8.48 (s, 1H), 8.06 (dd, *J* = 9.4, 1.5 Hz, 1H), 7.89 (d, *J* = 9.3 Hz, 1H), 7.85 (d, *J* = 8.0 Hz, 2H), 7.58 (dd, *J* = 8.2, 1.6 Hz, 2H), 4.69 (dd, *J* = 57.4, 8.4 Hz, 1H), 4.58 (dd, *J* = 13.8 Hz, 8.4 Hz, 1H), 4.52–3.74 (m, 6H), 2.96 (s, 3H), 2.94 (d, *J* = 1.1 Hz, 3H), 2.82–2.44 (m, 2H).

(2S,3S)-3-Amino-4-(3,3-difluoropyrrolidin-1-yl)-*N,N*-dimethyl-4-oxo-2-(4-[1,2,4]triazolo[1,5-*a*]pyridin-6-ylphenyl)butanamide Hydrochloride (6b). The *tert*-butyl [(1S,2S)-1-[(3,3-difluoropyrrolidin-1-yl)carbamoyl]-3-(dimethylamino)-3-oxo-2-(4-[1,2,4]triazolo[1,5-*a*]pyridin-6-yl)propyl]carbamate (6.9 g,

12.7 mmol) was dissolved in a 1:1 mixture of dichloromethane and TFA, stirred for 30 min at room temperature, then concentrated in vacuo. The TFA salt was then dissolved in water, and the aqueous solution adjusted to pH 9 via addition of 2 N aqueous sodium carbonate solution. After extracting the aqueous mixture with 3:1 chloroform:2-propanol (5 × 200 mL), the combined organic layers were washed once with brine, then dried over sodium sulfate, filtered, and concentrated in vacuo. The resultant free base was then dissolved in dichloromethane, and 30 mL of 2 N hydrogen chloride in ether was added to the solution. After stirring for 60 min, the solution was evaporated to afford the title compound as a white hydrochloride salt. The compound was further purified by recrystallization from ethanol/ether. Lyophilization of the recrystallized compound from water/acetonitrile (40:60, 100 mL) then afforded **6b** as a fluffy white crystalline solid (3.7 g, 61% yield). 100% purity by HPLC (Method B, *t_r* = 7.25 min); LC/MS *m/e* 443.2 (M + H)⁺; HRMS (ES⁺) calcd for C₂₂H₂₅F₂N₆O₂ (M + H)⁺ *m/e* 443.2007, found *m/e* 443.2003. ¹H NMR (500 MHz, CD₃OD) δ 9.12 (s, 1H), 8.48 (s, 1H), 8.06 (dd, *J* = 9.4, 1.6 Hz, 1H), 7.87 (d, *J* = 9.3 Hz, 1H), 7.85 (d, *J* = 8.0 Hz, 2H), 7.58 (dd, *J* = 8.2, 1.6 Hz, 2H), 4.69 (dd, *J* = 57.4, 8.4 Hz, 1H), 4.58 (dd, *J* = 13.8, 8.2 Hz, 1H), 4.52–3.74 (m, 6H), 2.96 (s, 3H), 2.94 (d, *J* = 1.1 Hz, 3H), 2.69–45 (m, 2H).

X-ray Crystallographic Analysis. DPP-4 (residues 39–766) was crystallized in the presence of compound **23** following the reported conditions.²² A 94.8% complete, 5.5-fold redundant X-ray diffraction data set to 2.4 Å was collected from a single-crystal cooled to 100 K, using the beamline 17-BM at the Advanced Photon Source (Argonne, IL). The structure was solved using Molecular Replacement procedures (MOLREP³⁶) and the 1N1M.pdb coordinate file, without water, ligand, and sugar molecules. The structure was refined against all available data to 2.4 Å, using CNX (Accelrys³⁷) to a crystallographic R-factor of 19.4% and an *R*_{free} of 24.0%. The root-mean-square deviation between the model and ideal bond distances and bond angles are 0.010 Å and 1.46°, respectively. Coordinates have been deposited with the Protein Data Bank, accession code 2FJP. Data collection and refinement statistics and further refinement details are available as Supporting Information.

Oral Glucose Tolerance Test in Lean Mice. Male C57BL/6N mice (7–12 weeks of age) from Taconic Farms, Germantown, NY were housed 10 per cage and given access to normal diet rodent chow (Teklad 7012) and water ad libitum. Mice (*n* = 7/group) were randomly assigned to treatment groups and fasted overnight (~18–21 h). Baseline (*t* = -60 min) blood glucose concentration was determined by glucometer from tail nick blood. Animals were then treated orally with vehicle (0.25% methylcellulose, 5 mL/kg) or compound **6b** (3, 1, 0.3 and 0.1 mg/kg; 5 mL/kg). Blood glucose concentration was measured 1 h after treatment (*t* = 0 min), and mice were then orally challenged with dextrose (5 g/kg, 10 mL/kg). One group of vehicle-treated mice was challenged with water as a negative control. Blood glucose levels were determined from tail bleeds taken 20, 40, 60, and 120 min after dextrose challenge. The blood glucose excursion profile from *t* = 0 to *t* = 120 min was used to integrate an area under the curve (AUC) for each treatment. Percent reduction values for each treatment were generated from the AUC data normalized to the water-challenged controls.

Lean Mouse Pharmacodynamic Assay. Male C57BL/6N mice (7–12 weeks of age, 19–26 g) from Taconic Farms, Germantown, NY, were housed 10 per cage and given access to normal diet rodent chow (Teklad 7012) and water ad libitum. Mice (*n* = 20–28/group) were randomly assigned to treatment groups and fasted overnight (~18–21 h). Baseline (*t* = -60 min) blood glucose concentration was determined by glucometer from tail nick blood. Animals were then treated orally with vehicle (0.25% methylcellulose, 5 mL/kg) or compound **6b** (3, 1, 0.3, and 0.1 mg/kg; 5 mL/kg) and the blood glucose concentration determined 1 h after treatment (*t* = 0 min). After the blood glucose determination at *t* = 0, mice were orally challenged with dextrose (5 g/kg, 10 mL/kg). One group of vehicle-treated mice was challenged with water as a negative control. Blood glucose levels were determined from tail bleeds taken 20 min after

dextrose challenge. Mice were then immediately euthanized and terminal blood samples collected by cardiac puncture. Blood samples were collected into EDTA, and the plasma was harvested by centrifugation. Aliquots of plasma samples were stored at -70°C until analysis.

Measurement of Plasma DPP-4 Activity.²⁹ Plasma DPP-4 activity was measured using a continuous fluorometric assay with the substrate Gly-Pro-AMC, which is cleaved by DPP-4 to release the fluorescent AMC leaving group. A typical reaction contains 50% plasma, 50 μM Gly-Pro-AMC, and buffer (100 mM HEPES, pH 7.5, 0.1 mg/mL BSA) in a total reaction volume of 50 to 70 μL (depending on the availability of sample). Liberation of AMC was monitored continuously in a 96-well plate fluorometer (SpectramAX Gemini, Molecular Devices), using an excitation wavelength of 360 nm and an emission wavelength of 460 nm. Under these conditions, approximately 5 μM AMC is produced in 5 min at 37°C . The plate reader used was a SpectramAX Gemini (Molecular Devices). The assay exhibits linear rates only for about 5 min due to the rapid substrate depletion. Therefore, it was important to preincubate all assay components to the assay temperature prior to the assay. The data are reported as % inhibition calculated as follows: %Inhibition = $100(1 - (V_t/V_c))$, where V_t is the rate of reaction of treated sample and V_c is the rate of reaction of control sample.

Measurement of Plasma active (intact) GLP-1. Plasma intact GLP-1 was measured using a 96-well ELISA kit for active hormone, purchased from Linco Research Inc (St. Charles, MO, cat. # EGPL-35K). The assay has a detection limit of 2 pM and is selective for active GLP-1 (GLP-1[7–36] amide and GLP-1[7–37]). The DPP-4 inhibitor valine thiazolidide (100 μM) was added to plasma aliquots for active GLP-1 measurements to prevent degradation of the hormone.

Determination of Plasma Concentration of Compound 6. Plasma concentrations of compound **6** were determined 20 min after dextrose challenge and 80 min postcompound administration by liquid chromatography/tandem mass spectrometry. Plasma was prepared for MS analysis by solid-phase extraction using OASIS-HLB 96-well extraction plates. The typical limit of quantitation was 10 nM.

Oral Glucose Tolerance Test in Diet Induced Obese (DIO) Mice. Male C57BL/6N mice were purchased from Taconic Farms, Germantown, NY. At 5 weeks of age they were placed on a high fat diet F-3282 (35% fat by weight) supplied by BioServ, NJ, for 27 weeks. An age-matched cohort of mice was fed a normal diet rodent chow (Teklad 7012) to provide a lean control group. All mice were given access to food and water ad libitum. At approximately 7 months of age, mice were used for the following OGTT. DIO animals were randomly assigned to treatment groups. The DIO (45–55 g) and lean mice (28–32 g) ($n = 7-8/\text{group}$) were fasted overnight (18–21 h), and baseline ($t = -60$ min) blood glucose concentration was determined by glucometer from tail nick blood. DIO animals were then treated orally with vehicle (0.25% methylcellulose, 5 mL/kg) or compound **6b** (30, 3, 0.3 mg/kg; 5 mL/kg). Lean control mice received only vehicle. Blood glucose concentration was measured 1 h after treatment ($t = 0$ min), and mice were then orally challenged with dextrose (2 g/kg, 10 mL/kg). Blood glucose levels were determined from tail bleeds taken 20, 40, 60, and 120 min after dextrose challenge. The blood glucose excursion profile from $t = 0$ to $t = 120$ min was used to integrate an area under the curve (AUC) for each treatment. Percent reduction values for each treatment were generated from the AUC data normalized to the dextrose-challenged lean controls.

Determination of Plasma Protein Binding of Compound 6a. [^3H]**6a** (0.5 and 20 μM) was incubated with a fresh pooled source of plasma from male CD-1 mouse, C57BL mouse, Sprague–Dawley rat, beagle dog, rhesus monkey, and human. Following incubations at 37°C for 30 min, an aliquot was counted for radioactivity, and duplicate 1 or 0.5 mL aliquots of plasma were transferred into centrifuge tubes and centrifuged at 100 000 rpm (Beckman centrifuge model TL-100, rotor TLA 100.2) at 37°C for 3 h. The centrifuge was stopped without braking to minimize

disturbance of samples. Four aliquots (200 or 100 μL) were taken sequentially from the top of the vial using narrow pipet tips and assayed for total radioactivity. The protein pellet (bottom layer) was digested by incubating with 8 M urea or 0.01 N NaOH and analyzed for total radioactivity by liquid scintillation counting. The unbound fraction was determined from the ratio of radioactivity in the protein free fraction to that in plasma prior to centrifugation. Recoveries were calculated by adding the total radioactivity measured in the different layers, including the protein pellet, and comparing that value to the radioactivity present in plasma before incubation.

Diltiazem/ Ca^{+2} L-type Channel Binding Assay. L-type Ca^{+2} binding was performed following a published procedure²⁷ using membranes prepared from rabbit skeletal muscle. Compounds were serially diluted in DMSO then mixed with ^3H -diltiazem (20 nM final concentration, NEN) and 40–70 μg membranes in assay buffer (50 mM Tris, pH 7.4). The assay was incubated for 60 min at room temperature with shaking. Following incubation, the membranes were harvested using a Packard Filtermate Harvester and GF/C filter plates that had been presoaked in 0.3% polyethylenimine (PEI). The plates were then washed three times with ice-cold assay buffer. Plates were then air-dried and counted in a Packard TopCounter. Total binding was determined in wells with DMSO only, and nonspecific binding was determined in the presence of 20 μM unlabeled diltiazem. Data analysis was performed using Microsoft Excel and GraphPad Prism software.

Cardiac Type-2 Na^{+2} Channel Binding Assay. Inhibition of binding to the human cardiac Na^{+} Channel (hNa_v 1.5, hH1a) was performed using membranes made from HEK293 cells stably expressing the channel as described in the literature.²⁸ Compounds were serially diluted in DMSO and added to ligand (^3H -BPBTS, 1 nM final concentration, MRL Compound Synthesis) and 40–80 μg of membranes in assay buffer (20 mM Tris-HCl, pH 7.4; 0.01 mg/mL Bacitracin). The assay was then incubated overnight (16 h) at room temperature with shaking. Following the incubation, a Packard Filtermate Harvester and GF/B filter plates (presoaked in 0.3% PEI) were used to harvest the membranes. The plates washed three times with ice-cold wash buffer (20 mM Tris, pH 7.4; 150 mM NaCl; 0.05% Triton X-100). The filter plates were then air-dried and counted in a Packard TopCount scintillation counter. Total binding was determined in wells with DMSO only, and nonspecific binding was determined in the presence of 5 μM unlabeled ligand. Data analysis was performed using Microsoft Excel and GraphPad Prism software.

Acknowledgment. The authors thank Dr. Philip Eskola, Daniel Kim, and Regina Black of Synthetic Services Group for large scale synthetic support. We also thank Dr. Bernard Choi and Falguni Patel for providing high-resolution mass spectral analyses. We thank W. P. Feeney, J. E. Fenyk-Melody, J. C. Hausamann, S. A. Iliff, C. N. Nunes, A. S. Parlapiano, G. M. Seeburger, X. Shen, and K. G. Vakerich for dosing the animals used in pharmacokinetic studies. Use of the beamline 17-BM with beamline management and support provided by staff from IMCA-CAT at the Advanced Photon Source was supported by the companies of the Industrial Macromolecular Crystallography Association through a contract with Illinois Institute of Technology. Use of the Advanced Photon Source was supported by the U.S. Department of Energy, Office of Science, Office of Basic Energy Sciences, under Contract No. W-31-109-Eng-38.

Supporting Information Available: The X-ray crystallographic data of compound **23** bound to DPP-4 are available. This material is available free of charge via the Internet at <http://pubs.acs.org>.

References

- (1) (a) Weber, A. E. Dipeptidyl Peptidase IV Inhibitors for the Treatment of Diabetes. *J. Med. Chem.* **2004**, *47*, 4135–4141. (b) Deacon, C. F.; Ahren, B.; Holst, J. J. Inhibitors of Dipeptidyl Peptidase IV: A Novel Approach for the Prevention and Treatment of Type 2

- Diabetes? *Expert Opin. Investig. Drugs* **2004**, *13*, 1091–1102. (c) Augustyns, K.; Veken, P. V. V.; Haemers, A. Inhibitors of Proline-Specific Dipeptidyl Peptidases: DPP-4 Inhibitors as a Novel Approach for the Treatment of Type 2 Diabetes. *Expert Opin. Ther. Patents* **2005**, *15*, 1387–1407.
- (2) (a) Ahren, B. E. Enhancement or Prolongation of GLP-1 Activity as a Strategy for Treatment of Type 2 Diabetes. *Drug Discovery Today: Ther. Strategies* **2004**, *1*, 207–212. (b) Deacon, C. F. Therapeutic Strategies Based on Glucagon-Like Peptide 1. *Diabetes* **2004**, *53*, 2181–2189. (c) Deacon, C. F.; Holst, J. J.; Glucagon-Like Peptide 1 and Inhibitors of Dipeptidyl Peptidase IV in the Treatment of Type 2 Diabetes Mellitus. *Curr. Opin. Pharmacology* **2004**, *4*, 589–596. (d) Mentlein, R. Therapeutic Assessment of Glucagon-like Peptide-1 Agonists Compared with Dipeptidyl Peptidase IV Inhibitors as Potential Antidiabetic Drugs. *Expert Opin. Invest. Drugs* **2005**, *14*, 57–64. (e) Nielsen, L. L. Incretin Mimetics and DPP-4 Inhibitors for the Treatment of Type 2 Diabetes. *Drug Discovery Today* **2005**, *10*, 703–710. (f) Gautier, J. F.; Fetita, S.; Sobngwi, E.; Salaun-Martin, C. Biological Actions of the Incretins GIP and GLP-1 and Therapeutic Perspectives in Patients with Type 2 Diabetes. *Diabetes Metab.* **2005**, *31*, 233–242.
- (3) (a) Villhauer, E. B.; Brinkman, J. A.; Naderi, G. B.; Burkey, B. F.; Dunning, B. E.; Prasad, K.; Mangold, B. L.; Russell, M. E.; Hughes, T. E. 1-[[[(3-Hydroxy-1-Adamantyl)amino]acetyl]-2-cyano-(S)-pyrrolidine: A Potent Selective, and Orally Bioavailable Dipeptidyl Peptidase IV Inhibitor with Antihyperglycemic Properties. *J. Med. Chem.* **2003**, *46*, 2774–2789. (b) Barlocco, D. LAF-237. *Curr. Opin. Investig. Drugs* **2004**, *5*, 1094–1100. (c) McIntyre, J. A.; Castaner, J. Vildagliptin. *Drugs Future* **2004**, *29*, 887–891.
- (4) Augeri, D. J.; Robl, J. A.; Betebenner, D. A.; Magnin, D. R.; Khanna, A.; Robertson, J. G.; Wang, A.; Simpkins, L. M.; Taunk, P.; Huang, Q.; Han, S.-P.; Abboa-Offei, B. E.; Cap, M.; Xin, L.; Tao, L.; Tozzo, E.; Welzel, G. E.; Egan, D. M.; Marcinkeviciene, J.; Chang, S. Y.; Biller, S. A.; Kirby, M. S.; Parker, R. A. and Hamann, L. G. Discovery and Preclinical Profile of Saxagliptin (BMS-477118): A Highly Potent, Long-Acting, Orally Active Dipeptidyl Peptidase IV Inhibitor for the Treatment of Type 2 Diabetes. *J. Med. Chem.* **2005**, *48*, 5025–5037.
- (5) Kim, D.; Wang, L.; Beconi, M.; Eiermann, G. J.; Fisher, M. H.; He, H.; Hickey, G. J.; Kowalchick, J. E.; Leiting, B.; Lyons, K.; Marsillio, F.; McCann, M. E.; Patel, R. A.; Petrov, A.; Scapin, G.; Patel, S. B.; Roy, R. S.; Wu, J. K.; Wyrvatt, M. J.; Zhang, B. B.; Zhu, L.; Thornberry, N. A.; Weber, A. E. (2R)-4-Oxo-4-[3-(trifluoromethyl)-5,6-dihydro[1,2,4]triazolo[4,3-a]pyrazin-7(8H)-yl]-1-(2,4,5-trifluorophenyl)butan-2-amine: A Potent, Orally Active Dipeptidyl Peptidase IV Inhibitor for the Treatment of Type 2 Diabetes. *J. Med. Chem.* **2005**, *48*, 141–151. (b) Deacon, C. F. MK-431 Merck. *Curr. Opin. Investig. Drugs* **2005**, *6*, 419–426. (c) Sorbera, L. A.; Castaner, J. MK-0431. *Drugs Future* **2005**, *30*, 337–343.
- (6) Another strategy to optimize the P-2 substituent as phenylalanine derivatives was recently reported, see Qiao, L.; Baumann, C. A.; Crysler, C. S.; Ninan, N. S.; Abad, M. C.; Spurlino, J. C.; DesJarlais, R. L.; Kervinen, J.; Nepper, M. P.; Bayoumy, S. S.; Williams, R.; Beckman, I. C.; Dasgupta, M.; Reed, R. L.; Huebert, N. D.; Tomczuk, B. E.; Moriarty, K. J. Discovery, SAR, and X-ray Structure of Novel Biaryl-Based Dipeptidyl Peptidase IV Inhibitors. *Bioorg. Med. Chem. Lett.* **2006**, *16*, 123.
- (7) (a) Xu, J.; Wei, L.; Mathvink, R.; He, J.; Park, Y.-J.; He, H.; Leiting, B.; Lyons, K. A.; Marsilio, F.; Patel, R. A.; Wu, J. K.; Thornberry, N. A.; Weber, A. E. Discovery of Potent and Selective Phenylalanine Based Dipeptidyl Peptidase IV Inhibitors. *Bioorg. Med. Chem. Lett.* **2005**, *15*, 2533–2536. (b) Edmondson, S. E.; Mastracchio, A.; Duffy, J. L.; Eiermann, G. J.; He, H.; Ita, I.; Leiting, B.; Leone, J. F.; Lyons, K. A.; Makarewicz, A. M.; Patel, R. A.; Petrov, A.; Wu, J. K.; Thornberry, N. A.; Weber, A. E. Discovery of Potent and Selective Orally Bioavailable β -Substituted Phenylalanine Derived Dipeptidyl Peptidase IV Inhibitors. *Bioorg. Med. Chem. Lett.* **2005**, *15*, 3048–3052.
- (8) Xu, J.; Wei, L.; Mathvink, R.; Edmondson, S. D.; Mastracchio, A.; Eiermann, G. J.; He, H.; Leone, J. F.; Lyons, K. A.; Marsilio, F.; Patel, R. A.; Wu, J. K.; Thornberry, N. A.; Weber, A. E. Discovery of Potent, Selective and Orally Bioavailable Pyridone Based Dipeptidyl Peptidase IV Inhibitors. *Bioorg. Med. Chem. Lett.* **2006**, *16*, 1346–1349.
- (9) Huntsman, E.; Balsells, J. New Method for the General Synthesis of [1,2,4]Triazolol[1,5-a]pyridines. *Eur. J. Org. Chem.* **2005**, 3761–3765.
- (10) Wu, Z.; Fraley, M. E.; Bilodeau, M. T.; Kaufman, M. L.; Tasber, E. S.; Balitza, A. E.; Hartman, G. D.; Coll, K. E.; Rickert, K.; Shipman, J.; Shi, B.; Sepp-Lorenzino, L.; Thomas, K. A. Design and Synthesis of 3,7-Diarylimidazopyridines as Inhibitors of the VEGF-Receptor KDR. *Bioorg. Med. Chem. Lett.* **2004**, *14*, 909–912.
- (11) (a) Corey, E. J.; Helal, C. J. Novel Electronic Effects of Remote Substituents on the Oxazaborolidine-Catalyzed Enantioselective Reduction of Ketones. *Tetrahedron Lett.* **1995**, *36*, 9153–9156. (b) Corey, E. J.; Bakshi, C. J. A New System for Catalytic Enantioselective Reduction of Achiral Ketones to Chiral Alcohols. Synthesis of Chiral α -Hydroxy Acids. *Tetrahedron Lett.* **1990**, *31*, 611–614.
- (12) Kazmaier, U. Synthesis of Unsaturated Amino Acids by [3,3]-Sigmatropic Rearrangement of Chelate-Bridged Glycine Ester Enolates. *Angew. Chem., Int. Ed. Engl.* **1994**, *33*, 998–999.
- (13) 3-Fluoroazetidone was synthesized by a procedure reported in Colandrea, V. J.; Edmondson, S. D.; Mathvink, R. J.; Mastracchio, A.; Weber, A. E.; Xu, J. Phenylalanine Derivatives as Dipeptidyl Peptidase Inhibitors for the Treatment or Prevention of Diabetes, Patent WO 04/043940, May 27, 2004.
- (14) Caldwell, C. G.; Chen, P.; He, J.; Parmee, E. R.; Leiting, B.; Marsilio, F.; Patel, R. A.; Wu, J. K.; Eiermann, G. J.; Petrov, A.; He, H.; Lyons, K. A.; Thornberry, N. A.; Weber, A. E. Fluoropyrrolidine Amides as Dipeptidyl Peptidase IV Inhibitors. *Bioorg. Med. Chem. Lett.* **2004**, *14*, 1265–1268.
- (15) For assay conditions see: Leiting, B.; Pryor, K. D.; Wu, J. K.; Marsilio, F.; Patel, R. A.; Craik, C. S.; Ellman, J. A.; Cummings, R. T.; Thornberry, N. A. Catalytic Properties and Inhibition of Proline-Specific Dipeptidyl Peptidases II, IV and VII. *Biochem. J.* **2003**, *371*, 525–532.
- (16) Abbot, C. A.; Yu, D. M.; Woollatt, E.; Sutherland, G. R.; McCaughan, G. W.; Gorrell, M. D. Cloning, Expression and Chromosomal Localization of a Novel Human Dipeptidyl Peptidase (DPP) IV Homolog, DPP8. *Eur. J. Biochem.* **2000b**, *267*, 6140–6150.
- (17) Olsen, C.; Wagtman, N. Identification and Characterization of Human DPP9, a Novel Homologue of Dipeptidyl Peptidase IV. *Gene* **2002**, *299*, 185–193.
- (18) Scallan, M. J.; Raj, B. K. M.; Calvo, B.; Garin-Chesa, P.; Sanz-Moncasi, M. P.; Healey, J. H.; Old, L. J.; Rettig, W. J. Molecular Cloning of Fibroblast Activation Protein Alpha, a Member of the Serine Protease Family Selectively Expressed in Stromal Fibroblast of Epithelial Cancers. *Proc. Natl. Acad. Sci. U.S.A.* **1994**, *91*, 5657–5661.
- (19) (a) Sedo, A.; Malik, R. Dipeptidyl Peptidase IV-Like Molecules: Homologous Proteins or Homologous Activities? *Biochim. Biophys. Acta* **2001**, *1550*, 107–116. (b) Rosenblum, J. S.; Kozarich, J. W. Prolyl Peptidases: A Serine Protease Subfamily with High Potential for Drug Discovery. *Curr. Opin. Chem. Biol.* **2003**, *7*, 496–504.
- (20) McDonald, J. K.; Leibach, F. H.; Grindeland, R. E.; Ellis, S. Purification of Dipeptidyl Aminopeptidase II (Dipeptidyl Arylamidase II) of the Anterior Pituitary Gland. *J. Bio. Chem.* **1968**, *243*, 4143–4150.
- (21) Lankas, G. R.; Leiting, B.; Sinha Roy, R.; Eiermann, G. J.; Biftu, T.; Chan, C.-C.; Edmondson, S. D.; Feeney, W. P.; He, H.; Ippolito, D. E.; Kim, D.; Lyons, K. A.; Ok, H. O.; Patel, R. A.; Petrov, A. N.; Pryor, K. A.; Qian, X.; Reigle, L.; Woods, A.; Wu, J. K.; Zaller, D.; Zhang, X.; Zhu, L.; Weber, A. E.; Thornberry, N. A. Dipeptidyl Peptidase IV Inhibition for the Treatment of Type 2 Diabetes: Potential Importance of Selectivity Over Dipeptidyl Peptidases 8 and 9. *Diabetes* **2005**, *54*, 2988–2994.
- (22) Rasmussen, H. B.; Branner, S.; Wiberg, F. C.; Wagtman, N. Crystal Structure of Human Dipeptidyl Peptidase IV/CD26 in Complex with a Substrate Analog. *Nat. Struct. Biol.* **2003**, *10*, 19–25.
- (23) Xu, S.; Zhu, B.; Teffera, Y.; Pan, D. E.; Caldwell, C. G.; Doss, G.; Stearns, R. A.; Evans, D. C.; Beconi, M. G. Metabolic Activation of Fluoropyrrolidine Dipeptidyl Peptidase-IV Inhibitors by Rat Liver Microsomes. *Drug Metab. Dispos.* **2005**, *33*, 121–130.
- (24) Evans, D. C.; Watt, A. P.; Nicoll-Griffith, D. A.; Baillie, T. A. Drug-Protein Adducts: An Industry Perspective on Minimizing the Potential for Drug Bioactivation in Drug Discovery and Development. *Chem. Res. Toxicol.* **2004**, *17*, 3–16.
- (25) The relationship of Cl_p to MRT and volume of distribution at steady state ($V_{d,ss}$) is $Cl_p = V_{d,ss}/MRT$. Compounds with high Cl_p rates may exhibit short or long MRTs, where short MRT compounds have small $V_{d,ss}$ while longer MRT values result from compounds distributing into tissue (i.e. large $V_{d,ss}$). Compounds **32** and **33** possess large $V_{d,ss}$ and also have relatively large MRT's. Pharmacokinetic parameters were analyzed with WATSON software (version 6.4.0.04 Innaphase Corp) by noncompartmental methods using formulas described in Gibaldi, M.; Perrier, D. *Pharmacokinetics*, 2nd ed.; Swarbrick, J., Ed; Marcel Dekker: New York, 1982; pp 409–449.
- (26) IC_{50} determinations for hERG was carried out as described in Friesen, R.; Wu.; Ducharme, Y.; Ball, R. G.; Blouin, M.; Boulet, L.; Cote, B.; Frenette, R.; Girard, M.; Guay, D.; Huang, Z.; Jones, T. R.; Laliberte, F.; Lynch, J. J.; Mancini, J.; Martins, E.; Masson, P.; Muise, E.; Pon, D. J.; Siegel, P. K. S.; Styhler, A.; Tsou, N. N.; Turner, M. J.; Young, R. N.; Girard, Y. Optimization of a Tertiary Alcohol Series

- of Phosphodiesterase-4 (PDE4) Inhibitors: Structure–Activity Relationship Related to PDE4 Inhibition and Human Ether-a-go-go Related Gene Potassium Channel Binding Affinity. *J. Med. Chem.* **2003**, *46*, 2413–2426.
- (27) IC₅₀ determinations for human cardiac sodium channel was carried out as described in (a) Hartmann, H. A.; Tiedeman, A. A.; Chen, S. F.; Brown, A. M.; Kirsch, G. E. Effects of III–IV Linker Mutations on Human Heart Na⁺ Channel Inactivation Gating. *Circ. Res.* **1994**, *75*, 114–122. (b) Priest, B. T.; Garcia, M. L.; Middleton, R. E.; Brochu, R. M.; Clark, S.; Dai, G.; Dick, I. E.; Felix, J. P.; Liu, C. J.; Reiser, B. S.; Schmalhofer, W. A.; Shao, P. P.; Tang, Y. S.; Chou, M. Z.; Kohler, M. G.; Smith, M. M.; Warren, V. A.; Williams, B. S.; Cohen, C. J.; Martin, W. J.; Meinke, P. T.; Parsons, W. H.; Wafford, K. A.; Kaczorowski, G. J. A Disubstituted Succinamide is a Potent Sodium Channel Blocker with Efficacy in a Rat Pain Model. *Biochemistry* **2004**, *43*, 9866–9876.
- (28) IC₅₀ determinations for rabbit calcium channel were carried out as described in Schoemaker, H.; Hicks, P.; Langer, S. Calcium Channel Receptor Binding Studies for Diltiazem and Its Major Metabolites: Functional Correlation to Inhibition of Portal Vein Myogenic Activity. *J. Cardiovasc. Pharm.* **1987**, *9*, 173–180.
- (29) It should be noted that the % inhibition as determined using the in vitro assay underestimates the % inhibition achieved in vivo, as compound **6** is a competitive, rapidly reversible inhibitor and assay of plasma DPP-4 activity requires (1) dilution of plasma which results in a dilution of the total inhibitor, and (2) presence of substrate that competes with inhibitor for binding to the enzyme.
- (30) Marguet, D.; Baggio, L.; Kobayashi, T.; Bernard, A.-M.; Pierres, M.; Nielsen, P. F.; Ribel, U.; Watanabe, T.; Drucker, D. J.; Wagtmann, N. Enhanced Insulin Secretion and Improved Glucose Tolerance in Mice Lacking CD26. *Proc. Natl. Acad. Sci. U.S.A.* **2000**, *97*, 6864–6879.
- (31) The correlation between free fraction inhibitor concentration and in vitro IC₅₀ measurements supports the observed OGTT glucose reduction profiles of highly plasma protein bound (>80%) phenylalanine-derived DPP-4 inhibitors such as compounds **4-6**, **23**, **32**, and **33** from this paper.
- (32) Tee, O. S.; Paventi, M. Kinetics and Mechanism of Bromination of 2-Pyridone and Related Derivatives in Aqueous Solution. *J. Am. Chem. Soc.* **1982**, *104*, 4142–4146.
- (33) Moran, D. B.; Morton, G. O.; Albright, J. D. Synthesis of (Pyridinyl)-1,2,4-triazolo[4,3,a]pyridines. *J. Heterocycl. Chem.* **1986**, *23*, 1071–1077.
- (34) Reimlinger, H.; Peiren, M. A.; Merenyi, R. Reaktionen des 3(5)-Amino-pyrazols mit α,β -Ungesättigten Estern. Darstellung und Charakterisierung Isomerer Oxo-dihydro-pyrazolo-pyrimidine. *Chem. Ber.* **1970**, *103*, 3252–3265.
- (35) Byth, K. F.; Cooper, N.; Culshaw, J. D.; Heaton, D. W.; Oakes, S. E.; Minshull, C. A.; Norman, R. A.; Paupit, R. A.; Tucker, J. A.; Breed, J.; Pannifer, A.; Rowsell, S.; Stanway, J. J.; Valentine, A. L.; Thomas, A. P. Imidazo[1,2-*b*]pyridazines: A Potent and Selective Class of Cyclin-Dependent Kinase Inhibitors. *Bioorg. Med. Chem. Lett.* **2004**, *14*, 2249–2252.
- (36) Vagin, A.; Teplyakov, A. MOLREP: An Automated Program for Molecular Replacement. *J. Appl. Crystallogr.* **1997**, *30*, 1022–1025.
- (37) Brunger, A. T.; Adams, P. D.; Clore, G. M.; DeLano, W. L.; Gros, P.; Grosse-Kunstleve, R. W.; Jiang, J.-S.; Kuszewski, J.; Nilges, M.; Pannu, N. S.; Read, R. J.; Rice, L. M.; Simonson, T.; Warren, G. L. Crystallography & NMR System: A New Software Suite for Macromolecular Structure Determination. *Acta Crystallogr.* **1988**, *D54*, 905–921.

JM060015T